

TOPICAL REVIEW • **OPEN ACCESS**

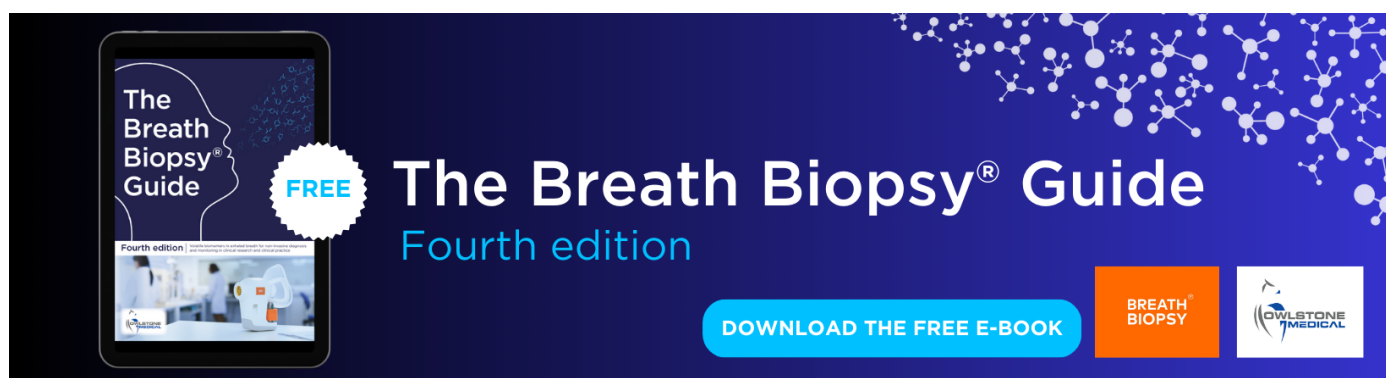
Recent development of respiratory rate measurement technologies

To cite this article: Haipeng Liu *et al* 2019 *Physiol. Meas.* **40** 07TR01

View the [article online](#) for updates and enhancements.

You may also like

- [Black holes, gravitational waves and fundamental physics: a roadmap](#)
Abbas Askar, Chris Belczynski, Gianfranco Bertone et al.
- [2021 roadmap on lithium sulfur batteries](#)
James B Robinson, Kai Xi, R Vasant Kumar et al.
- [2021 roadmap for sodium-ion batteries](#)
Nuria Tapia-Ruiz, A Robert Armstrong, Hande Alptekin et al.



The Breath Biopsy® Guide
Fourth edition

FREE

DOWNLOAD THE FREE E-BOOK

BREATH BIOPSY

OWLSTONE MEDICAL

OPEN ACCESS



TOPICAL REVIEW

Recent development of respiratory rate measurement technologies

RECEIVED
20 January 2019REVISED
4 April 2019ACCEPTED FOR PUBLICATION
13 June 2019PUBLISHED
2 August 2019

Original content from
this work may be used
under the terms of the
[Creative Commons
Attribution 3.0 licence](#).

Any further distribution
of this work must
maintain attribution
to the author(s) and the
title of the work, journal
citation and DOI.

Haipeng Liu^{1,2}, John Allen^{3,4}, Dingchang Zheng¹ and Fei Chen²¹ Faculty of Health, Education, Medicine, and Social Care, Anglia Ruskin University, Chelmsford, CM1 1SQ, United Kingdom² Department of Electrical and Electronic Engineering, Southern University of Science and Technology, Shenzhen 518055, People's Republic of China³ Institute of Cellular Medicine, Newcastle University, Newcastle upon Tyne NE2 4HH, United Kingdom⁴ Northern Medical Physics and Clinical Engineering, Newcastle upon Tyne NHS Foundation Trust, Newcastle upon Tyne NE7 7DN, United KingdomE-mail: dingchang.zheng@anglia.ac.uk, fchen@sustc.edu.cn and fchen@sustech.edu.cn**Keywords:** respiratory rate, wearable sensor, portable physiological measurement**Abstract**

Respiratory rate (RR) is an important physiological parameter whose abnormality has been regarded as an important indicator of serious illness. In order to make RR monitoring simple to perform, reliable and accurate, many different methods have been proposed for such automatic monitoring. According to the theory of respiratory rate extraction, methods are categorized into three modalities: extracting RR from other physiological signals, RR measurement based on respiratory movements, and RR measurement based on airflow. The merits and limitations of each method are highlighted and discussed. In addition, current works are summarized to suggest key directions for the development of future RR monitoring methodologies.

1. Introduction

Respiration involves a complex interaction between the central nervous system, respiration-related motor neurons, and the muscles of respiration (Sowho *et al* 2014). The effectiveness of the respiratory system also depends on the circulatory system (heart and blood vessels) (Elstad *et al* 2018). The central nervous system is responsible for determining respiratory drive in accordance to the input from peripheral and central chemoreceptors e.g. lungs, central chemoreceptors (pH), carotid and aortic chemoreceptors (CO₂ and O₂), and baroreceptors (blood pressure) (Mitchell 2004). Respiration-related motor neurons innervate the respiratory pump muscles to control alveolar ventilation (the production of respiratory rate and tidal volume) based on the input of central nervous system (Sowho *et al* 2014). Should hypoxaemia and hypercarbia be sensed by the peripheral and central chemoreceptors then respiratory rate (RR) and tidal volume are regulated to deliver oxygen to the pulmonary and systemic circulation and eliminate carbon dioxide from the lungs to return the system to the equilibrate state.

Clinically, RR is generally defined as the times of respiration observed during a minute (in breaths per minute, or bpm). RR is a vital sign whose abnormality is an important indicator of serious clinical events. Any derangement in the body system that causes hypoxaemia or hypercarbia could be detected by measuring RR. There is substantial evidence showing that an abnormal respiratory rate is a predictor of such potentially serious clinical events as intensive care unit (ICU) readmission (Cardoso *et al* 2014, Mlgaard *et al* 2016), cardiopulmonary arrest (Hodgetts *et al* 2002, Maharaj *et al* 2015), chronic heart failure (Ponikowski *et al* 2001a, 2001b, 2001c), pneumonia (Rambaud-Althaus *et al* 2015), pulmonary embolism (Egermayer *et al* 1998, Galle *et al* 2001, Jiménez *et al* 2016), weaning failure (Emidio Jorge 2013), and overdose (Hochhausen *et al* 2018). RR is a better discriminator than blood pressure and pulse rate in identifying high-risk patient groups of cardio-pulmonary catastrophic deterioration, since relative changes in RR are of a much greater magnitude and are therefore more likely to be better at discriminating between stable patients and patients at risk (Subbe *et al* 2003). This result was also supported by the research of Buist *et al* which suggested that an abnormal RR (<6 bpm or >24 bpm) is a stronger predictor of mortality than heart rate or hypertension (Buist *et al* 2004). A subtle deviation of RR as 4 bpm from the normal range could indicate an imminent medical emergency such as cardiac arrest due to cerebral hypoxia (Flenady *et al* 2017). More importantly, abnormal RR is a common feature hours before serious deterioration

Table 1. Current mainstream methods used for clinical RR monitoring.

Methods	Advantages	Limitations
Manual counting	Easy to perform, non-contact	Inaccurate, time-consuming
Spirometer	Accurate, simultaneous measurement of multiple respiratory parameters	Interfere with natural breathing Difficult for continuous RR monitoring
Capnometry	Accurate, easy to perform, able for continuous RR monitoring, simultaneous measurement of biochemical parameters.	Uncomfortableness caused by contact, special devices needed for analysis
Impedance pneumography	Accurate, continuous, simultaneous measurement of multiple respiratory parameters	Difficult to perform, special devices needed for analysis

and consequent cardiac arrest (Smith and Wood 1998). Hypoxaemia and hypercarbia do not always increase RR and tidal volume. Medications such as opiates and anaesthetics depress the respiratory drive and the respiratory response to hypoxia and hypercarbia. In this case, RR monitoring is very important in the safe and effective administration of anaesthesia, since the lowered RR often reflects the reduced consciousness (Cretikos *et al* 2008, Ermer *et al* 2017). Due to its potential in the early detection of patient deterioration, respiratory rate has been introduced to a range of early warning systems (Subbe *et al* 2001, Prytherch *et al* 2010, Williams *et al* 2012).

Although RR is clinically a strong indicator of serious events, RR measurement is still widely performed by manual counting with inaccurate results (Kellett *et al* 2011), or neglected (Flenady *et al* 2017). Research has indicated that RR measurement by nursing staff could be unreliable (Edmonds *et al* 2002, Lim *et al* 2002, Lovett *et al* 2005, Bianchi *et al* 2013, Flenady *et al* 2017). RR was often not recorded routinely, even when the patient's primary problem is a respiratory condition (Smith and Wood 1998, Edwards and Mordin 2001, Chellel *et al* 2002, Helliwell *et al* 2002, Hodgetts *et al* 2002, Hudson 2004, Ryan *et al* 2004, McBride *et al* 2005, Hogan 2006), possibly due to the unreliable results and poor compliance with timely procedures in a busy triage setting (Bianchi *et al* 2013). Considering the reliable monitoring of other vital signs such as heart rate and blood pressure, which can be automatically performed using simple electronic devices (Edwards and Mordin 2001), it is reasonable to deduce that the lack of a reliable automated RR monitor system contributes to the unsatisfactory situation of patients' RR monitoring (McBride *et al* 2005).

Clinically, RR could be recorded with a range of techniques, including spirometry, capnometry, and pneumography, as listed in table 1. These techniques often require cumbersome and expensive devices that may interfere with natural breathing, and can be unmanageable in certain applications such as ambulatory monitoring, stress testing, and sleep studies (Bailón *et al* 2006). Automatic, reliable and convenient sensors and devices could largely improve the situation of RR monitoring.

In recent years, owing to the technical improvements and prolonged lifespan, the development of medical devices has gained power. RR could be monitored automatically by the electronic monitors, with various benefits in pathological and physiological applications. Automatic RR monitoring could predict potentially serious clinical events such as cardiac arrest or admission to the ICU. The deviations of RR from the normal range during the measurement can be identified as high risk up to 24 h before the event with a specificity of 95% (Al-Khalidi *et al* 2011). Automatic RR monitoring is more sensitive than manual methods in detecting tachypnea (Kellett *et al* 2011, Bianchi *et al* 2013). In sleep studies, automatic RR monitoring could improve the diagnosis of apnea, which currently depends heavily on the expensive polysomnogram (Bailón *et al* 2006, Schöbel *et al* 2018).

Automatic respiratory monitoring devices are in urgent need to improve the clinical RR monitoring. In recent years, many automatic RR monitoring methods have been proposed. Based on different mechanisms, these methods are on different stages of development with different advantages and limitations. This review aimed to provide a technical overview of mainstream emerging methods of automatic RR monitoring.

2. Methods of respiratory rate measurement

In this section, the automatic respiratory rate measurement methods are reviewed. The approach for literature search was introduced. The methods were technically classified by their mechanisms (hardware and algorithm), with the operational process, the advantages, the limitations, and major applications discussed.

2.1. Literature search strategy

2.1.1. Preliminary search

This literature review includes published works that have been peer-reviewed. Our search was mainly focused on articles in journals, chapters of periodicals and proceedings of conferences written in English published between 2000 and 2018. We firstly searched on Google Scholar search engine with key words 'respiratory rate', 'respiration rate', 'breathing rate', 'tachypnea', or 'apnea', in combination with 'measurement', 'monitoring',

‘detection’, ‘estimation’, ‘wearable devices’, or ‘extraction’. More than 800 papers were found. From the titles of the works, technical keywords were extracted including electrocardiogram (ECG), photoplethysmogram (PPG), radar, thermal imaging, and others.

2.1.2. Technical categorization

Due to the large quantity of literature, categorization was firstly performed based on the technical keywords, as shown in the titles of sections from 2.2.1–2.4.3. These techniques were then categorized into the methods based on the respiratory modulation on other physiological signals (section 2.2), methods based on volume changes and body movement (section 2.3), and methods based on airflow changes (section 2.4).

2.1.3. Categorized search

For each technique, searches were conducted with its technical keyword combining the keywords in the preliminary search, on PubMed, IEEE Xplore, ACM Digital Library, and Google Scholar, between 2000 and 2018. The latest 20 papers were selected for each technique. The selected papers were checked to filter out some duplicated works, or following-up works with identical technical basis. For ECG and PPG, due to the large quantity of papers in the last five years, we chose the review papers and preserved some of the newest original algorithmic studies only. Finally, 235 papers were included in this review.

2.2. Methods based on the respiratory modulation on other physiological signals

With subjects periodically inhaling and exhaling, there are significant respiratory influences on physiological signals such as ECG, PPG, ballistocardiogram (BCG), seismocardiogram (SCG), osillometric cuff pressure pulses (OscP) and Korotkoff sounds (KorS), which are measured by electronic devices for different clinical applications. ECG records the electrical activity of the heart. PPG reflects the volumetric changes in blood in peripheral circulation. BCG is a measurement of the recoil forces of the body in reaction to cardiac ejection of blood into the vasculature while the seismocardiogram (SCG) represents the local vibrations of the chest wall in response to the heartbeat (Inan *et al* 2015). The OscP and KorS are the oscillometric and auscultatory methods that are widely used for blood pressure measurement (Chen *et al* 2016b). All these signals are modulated by respiration in various ways. Therefore RR could be estimated by the algorithms based on respiratory modulation. Compared with other methods, the RR estimation based on respiratory modulation of other physiological signals is less expensive, non-invasive and convenient, as RR could be measured simultaneously without adding extra instrumentation. In this section, RR extraction methods based on the respiratory modulation phenomenon will be detailed.

2.2.1. Mechanisms of respiratory modulation on ECG, PPG, BCG, SCG, OscP and KorS

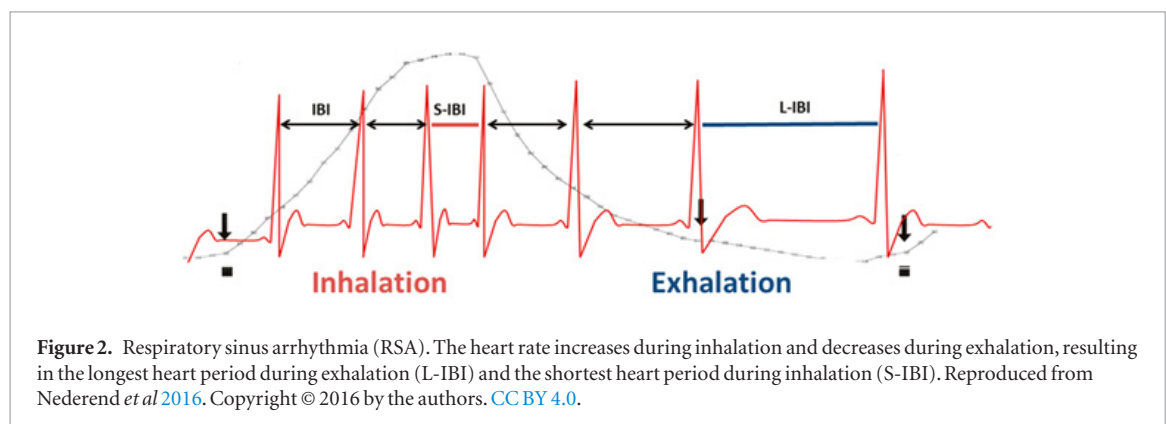
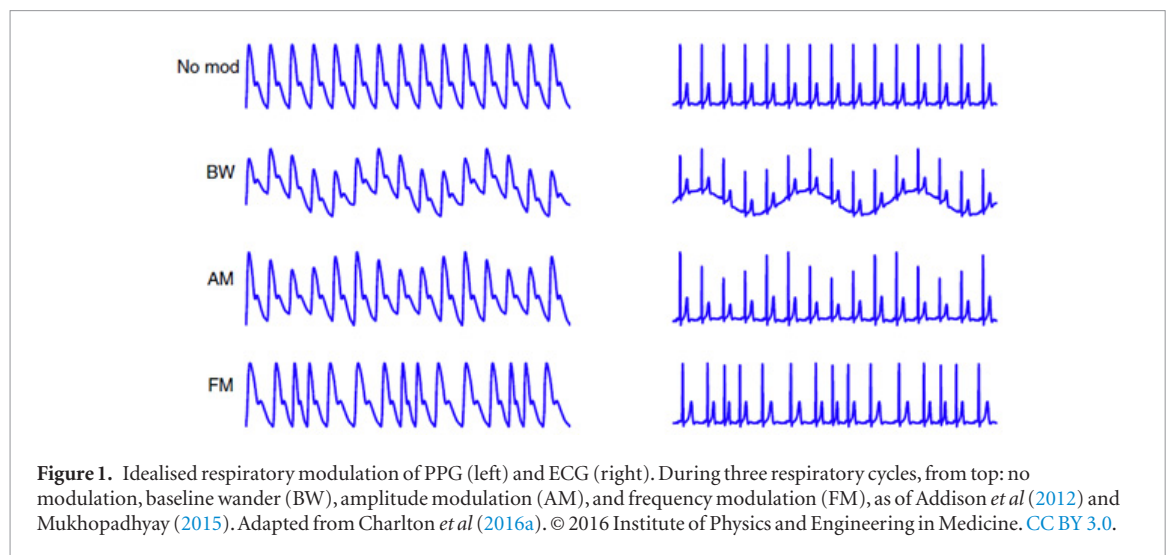
Respiratory modulations of ECG, PPG, BCG, SCG, OscP and KorS have different physiological mechanisms. For a certain signal, its amplitude, baseline, waveform, and frequency could be changed during inhalation and exhalation (figure 1). During inspiration, the apex of the heart moves towards the abdomen due to diaphragm contraction, whereas during expiration, the apex moves upwards (O’Brien and Heneghan 2007). Consequently, the periodic changes of transthoracic impedance and positions of the ECG electrodes relative to the heart (Clifford *et al* 2006, O’Brien and Heneghan 2007) result in the morphological changes, amplitude modulation (AM) and baseline wander (BW) of the ECG signal.

Although the mechanisms of the PPG signal have not been fully understood, it was observed that respiration directly influences the fluctuations in venous return, stroke volume, and arterial blood pressure, resulting in AM and BW of PPG (Meredith *et al* 2012), as shown in figure 1.

Reflecting the minor body movements caused by cardiorespiratory effects, BCG and SCG are composed of several independent peaks. These peaks indicate the cardiovascular activities in different phases of a cardiac cycle. By changing the position and amplitude of these peaks, respiration influences the waveform and amplitude of BCG and SCG (Pandia *et al* 2012, Alamdari *et al* 2016).

Similar to PPG, the tissue volume changes the pressure of the OscP measurement site, which is reflected on the amplitude of OscP signal. Despite the debated genesis of Korotkoff sounds, it is widely supposed that KorS is generated by the distension of the arterial wall caused by the changing transmural pressure gradient (McCutcheon and Rushmer 1967, Tavel *et al* 1969, Ur and Gordon 1970, Venet *et al* 2000). The respiratory modulation of stroke volume will directly influence the force deployed in opening the artery and consequently the blood flow sound, reflected by the amplitude of the KorS signal. Experiment results also showed the existence of amplitude modulation on OscP and KorS by respiration (Zheng *et al* 2014, Chen *et al* 2016a).

Frequency modulation effect, which exists commonly in ECG, PPG, BCG, SCG, OscP and KorS, is based on the respiratory sinus arrhythmia (RSA) in which the heart rate variation is associated with respiration, as shown in figure 2. Heart rate (HR) accelerates during inspiration and slows down during expiration (Yasuma and Hayano 2004, Grossman and Taylor 2007). This is a cardiorespiratory phenomenon universally observed among



vertebrates (Yasuma and Hayano 2004). HR could be demodulated from many physiological signals, enabling the extraction of RR (figure 1).

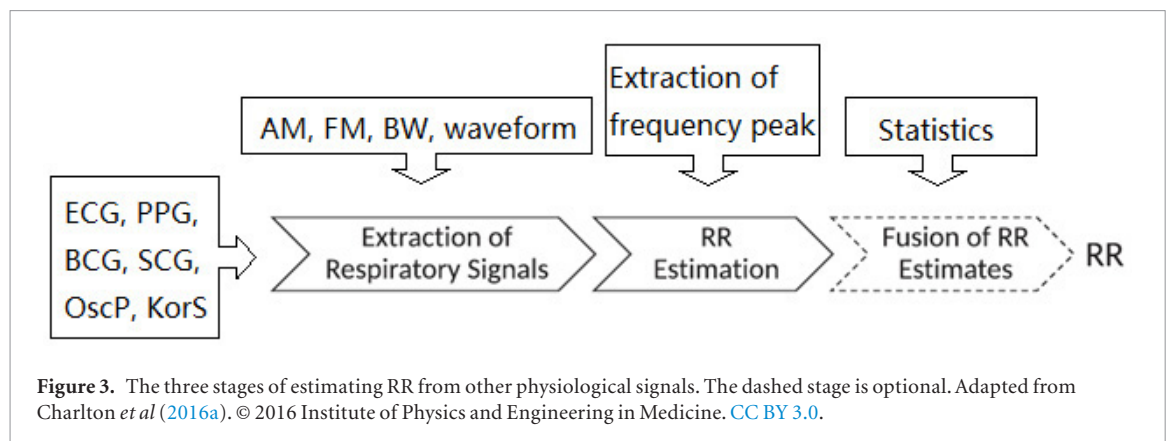
2.2.2. Algorithms for respiratory rate extraction from ECG, PPG, BCG, SCG, OscP and KorS

2.2.2.1. General process of RR extraction

Theoretically, the respiratory rate can be derived from the variations in the amplitudes or the beat-to-beat intervals of a physiological signal if the heart rate is at least two times greater than the respiration rate, which is often the case. Based on this, many algorithms have been proposed for extracting RR from ECG, PPG, BCG, SCG, OscP and KorS. Algorithms can be divided into three stages: extraction of respiratory signals, estimation of respiratory rate, and fusion of estimates (figure 3) (Mukhopadhyay 2015, Charlton *et al* 2016a).

In the first stage, the respiratory signal could be extracted by AM, FM, BW, and the changes in waveform between cardiac cycles caused by respiration. The techniques are often applicable to all the six signals since they are all primarily cardiac in origin, with secondary respiratory modulations of much lower magnitude (Mukhopadhyay 2015). The extraction could be feature- or filter-based. A systematical evaluation of major algorithms on RR extraction from ECG and PPG indicated that for respiratory signal extraction, feature-based technologies performed better than filter-based technologies (Charlton *et al* 2016a). Therefore, feature-based technologies were adopted by most of the top ranked methods (Charlton *et al* 2016a). Feature-based extraction of a respiratory signal is based on the time series of beat-by-beat feature measurements. Beat detection is typically performed using a segmentation algorithm (such as that proposed by Li *et al* (2010) for PPG signals and Pan and Tompkins (1985) for ECG signals). To derive the respiratory signal, the AM, FM and BW methods are then performed by measuring the pulse peak-to-trough amplitude (Karlen *et al* 2013), the beat-to-beat intervals (between consecutive fiducial points such as pulse peaks (Orphanidou *et al* 2013)), and the composite of pulse peak and trough amplitudes (Ruangsuwana *et al* 2010, Karlen *et al* 2013). Filter-based extraction consists of filtering the raw signal to attenuate non-respiratory frequency components, which is typically performed using a band-pass filter (Lindberg *et al* 1992), continuous wavelet transform (Addison and Watson 2004, Lin *et al* 2017) and a centred-correntropy function, which incorporates the time structure and statistical distribution of a signal (Garde *et al* 2014).

In the second stage, RR could be derived from the respiratory signal in the time or the frequency domains. The time-domain breath-detection techniques performed better than frequency-domain techniques, and were



therefore applied in top-ranked algorithms to estimate RR (Charlton *et al* 2016a). Frequency-domain techniques are commonly used but require evenly sampled data. Consequently, respiratory signals are often re-sampled onto an even grid prior to frequency-domain analysis. Fourier analysis has been used to calculate the frequency spectra of respiratory signals, from which the RR could be typically identified as the frequency peak corresponding to the maximum spectral power (Garde *et al* 2014). When RR is non-stationary across the window of data analyzed, the short-time Fourier transform (STFT) has been proposed to improve the accuracy of RR estimation (Shelley *et al* 2006a). A study comparing various algorithms extracting RR from PPG derived by the built-in cameras of smartphones and tablets indicated that the accuracy of all the algorithms decreased when RR was higher than 26 bpm (Nam *et al* 2014). Autoregressive (AR) modelling has been used to identify the resonant frequencies contained within a respiratory signal, with the accuracy improved for high RR extraction (Lee and Chon 2010).

The final step is to fuse RR estimates derived from different signals or by different algorithms. Firstly, for a certain physiological signal, the estimates derived by different modulations could be fused. The magnitude of each respiratory modulation may differ between individuals and physiological conditions. For example, the FM and AM derived the best RR estimation from the PPG signal respectively under resting and motion states (Shen *et al* 2017). Therefore averaging all RR estimates with different accuracies could hardly improve the overall accuracy. The error in RR estimation reached 3 bpm using the averaged value of RRs derived by AM, FM, and BW of PPG signal (Karlen *et al* 2013). However, after selecting the respiratory-related morphological parameters from the SCG signal, the averaged value could achieve the bias of -0.42 bpm compared with the reference RR derived by the respiratory belt (Pandia *et al* 2012). Some fusion methods based on signal quality have been proposed such as discarding the averaged RR if the range of RRs derived from FM, AM, and BW is greater than 4 bpm (Charlton *et al* 2016b), selecting the RR derived from ECG or PPG with the least temporal fluctuations within 60 s (Orphanidou 2017), adopting the RR value which appeared in more than half of the thirteen PPG-derived respiratory signals, or adopting the averaged RR value after removing the outliers (Cernat *et al* 2015). More advanced fusion methods were based on the statistical and probabilistic characteristics of signals such as the fusion of RRs derived from PPG signal by AM, FM, and BW with Gaussian process regression (Pimentel *et al* 2015).

Furthermore, the fusion could be performed between RRs estimated from different signals or measured by different sensors. Machine learning methods, such as linear regression (LR), supporting vector regression (SVR) and principal component analysis (PCA) could be applied in fusing the respiratory quality indices (RQI) derived from ECG and PPG signals by AM, FM, and BW (Birrenkott *et al* 2018). The fusion of RRs derived from the FM, AM, and BW of PPG, and from the accelerometer and gyroscope, could be fulfilled under static and running states by naive Bayes inference and static Kalman filter (Shen *et al* 2017). Referring to the standard RR value measured by respiratory belt, the fusion of RRs of accelerometer and gyro-senso by Kalman filter improved the estimating accuracy by 4.6% to 9.5% compared with the accelerometer-derived RR (Yoon *et al* 2014). The fusion of RR derived from ECG, PPG, and accelerometers could be fulfilled by selecting the most accurate estimate under different physiological states according to the features of three methods, with RR errors within 4.4% compared with the gold standard of capnometry (Liu *et al* 2013).

2.2.2.2. Algorithms based on ECG

The RR extraction from ECG has been developed for decades, and has more algorithms with higher accuracy when compared with PPG-based methods (Charlton *et al* 2016a). Thirteen different algorithms for detection of the sleep apnea by RR extracted from ECG recordings were analyzed in Penzel *et al* (2002). The best algorithms made use of the frequency-domain features to estimate the changes in the heart rate and the effect of respiration on the ECG waveform. For the ECG signal, FM often derived more accurate RR compared with AM (Orphanidou 2017). Algorithms based on the FM of ECG could be fulfilled on smartphones for the portable and continuous RR monitoring (Crema *et al* 2017). However, as the physiological basis of FM, RSA is reduced in the elderly, but the ECG waveform variability exists regardless of age, possibly more applicable for RR extraction (Trobec *et al* 2012).

Morphologically, the QRS wave of ECG is easy to extract to get the respiratory signal by AM. The high-frequency fluctuations of ECG reflect the respiratory effect on the muscle electric activity from which the respiratory signal could be derived by high-pass filtering (Helfenbein *et al* 2014). Other algorithms to derive respiratory signal from ECG include discrete Fourier transform (DFT) and the discrete cosine transform (DCT) based on morphological filtering, with better accuracy of RR estimation compared with the AM of R wave (Sharma *et al* 2015). The RR derived from FM and morphological parameters could reflect the effect of schizophrenia on the breathing pattern (Schmidt *et al* 2017). Based on the instantaneous values of the ECG-derived cardiac cycle length (R-R interval) and the dynamics of the cardiac cycle length series, the hidden Markov model and hidden semi-Markov model could be used for instant detection of apnea-bradycardia (Altuve *et al* 2012).

2.2.2.3. Algorithms based on PPG

PPG enabled the automated and continuous RR home-monitoring for the clinical screening of asthma, sleep apnea, and cardiovascular risks (Charlton *et al* 2016b). Many signal processing and machine learning techniques have been proposed for the estimation of RR from the PPG, including digital filter, short-time Fourier transform (STFT), continuous wavelet transform (CWT), empirical mode decomposition (EMD) and neural network (NN), independent component analysis (ICA), modified multi-scale principal component analysis (MMSPCA), variable-frequency complex demodulation (VFCDM), the autoregressive (AR) model, particle filter combining both time-invariant (TIV) and time-varying autoregressive (TVAR) models, pulse width variability, probabilistic approach, correntropy spectral density (CSD), and sparse signal reconstruction (SSR) in the spectral domain with RR tracking (RRT) then selects the most appropriate frequency component based on the previous RR (Ambekar and Prabhu 2015, Zhang and Ding 2016). Signal quality index (SQI), which reflects the presence of artefact in the signal, and respiratory quality indices (RQIs), which reflects exclusively the respiratory effect, were introduced into the pre-processing of PPG signal to enhance its quality for RR estimation (Birrenkott *et al* 2016). With decreased sampling frequency (Nam *et al* 2014), PPG signal could be derived on smartphones by contact detection on the finger, and by non-contact detection with imaging analysis (Papon *et al* 2015). Based on wavelet analysis, the automatic threshold selection of modified multiscale principal component analysis (MMSPCA) could extract a respiratory signal from short-length PPG signals (Motin *et al* 2017). The AM-based wavelet algorithms could derive RR from PPG and can be embedded in the micro-controller (MCU) of a pulse oximeter, creating the instantaneous RR monitoring (Lin *et al* 2017), which is applicable for clinical low-acuity care (Bergese *et al* 2017). Besides RR, the tidal volume could further be estimated from PPG using a recurrent neural network (Prinable *et al* 2017). However, considering the decreased intensity of PPG-derived respiratory signal with increasing RR, high RR is difficult to accurately detect from PPG signal by both FM and AM (Nam *et al* 2016a). The fusion of FM, AM, and pulse wave parameters enhanced the accuracy of PPG-based RR estimation on different smartphone devices (iPhone 4S, iPod 5, and HTC One M8). But the performance still degraded at higher rates (up to 30 bpm when using HTC One M8, and up to 36 bpm when using the iPhone 4S or iPod 5 devices) (Lázaro *et al* 2015). On smartphones and tablets, RRs derived from PPG signal by the autoregressive (AR) model, variable-frequency complex demodulation (VFCDM), and continuous wavelet transform (CWT) all indicated good accordance with the reference RR measured by a chest strap, but deviated from the reference value in high RR range (Nam *et al* 2014). Another unsolved issue was the differences between body sites in PPG-derived respiratory signal. It was observed that finger PPG derived better respiratory signals than ear PPG, and the respiratory signal from the arm was better than that from the forehead (Charlton *et al* 2017). This was due to the different ratios between cardiac and respiratory components of PPG signal on different body sites (Nilsson *et al* 2007). The frequency spectral analysis of PPG signal showed that respiratory signal from the forehead was at least ten times greater in intensity than that from the finger site (Shelley *et al* 2006b). However, Mayer waves are close to 0.1 Hz and strongly affect the PPG-derived respiratory signal from the forehead since it generates noise of ~0.1–0.2 Hz thereby at risk of disabling the reliability of RR extraction, while the finger was largely unaffected (Hernando *et al* 2017). Finally, PPG is afflicted by motion artifacts whose frequency band (usually below 0.2 Hz) overlaps respiratory frequencies (0.2–0.4 Hz). The modified multi-scale principal component analysis (MMSPCA) was proposed to extract respiratory signal from the PPG signal even with strong motion artifacts (Madhav *et al* 2013).

2.2.2.4. Algorithms based on BCG and SCG

Both BCG and SCG are three-dimensional (3D) in essence, but are often measured along the head-to-toe and dorsal-ventral directions respectively (Inan *et al* 2015). The location and direction of the sensor are therefore important for accurate BCG and SCG recording, but were often neglected (Inan *et al* 2015). BCG is influenced by the position and respiration (especially the residue volume during apnea), and is sensitive to the gravity (Martín-Yebra *et al* 2017) and motion artifacts (Hermann *et al* 2018). Despite the difference in waveform, BCG signals of different body sites were available for RR extraction (Vehkaoja *et al* 2015). Especially, the BCG estimation could be fulfilled on the sites such as behind the ear for portable RR monitoring (Da He *et al* 2010).

Currently, investigations on BCG and SCG mainly focused on the cardiac instead of respiratory effects. By combining different respiratory modulations on morphology and the frequency of SCG, the bias of derived RR in comparison with the reference value measured by the respiratory strap was -0.42 bpm, indicating that SCG is potential for RR monitoring (Pandia *et al* 2012). Two accelerometer-derived respiration (ADR) signals could be calculated by AM from the upper and lower envelopes of the SCG. By morphological analysis, a metric so-called the piecewise total harmonic distortion (THD) could identify which one of the lower and upper envelopes was the best ADR for detecting respiratory phases of the subject. The accuracy of piecewise THD in the selection of the correct envelope of SCG signal as an estimation of ADR was 84.6% (Alamdari *et al* 2016). The extraction of respiratory phase from SCG based on a support vector machine (SVM) algorithm showed that the time-domain features of SCG waveform (indicating the open and close of aortic valve, the cardiac cycle length) indicated higher total accuracies compared to other features (Zakeri *et al* 2016).

The wearable measurement of BCG and SCG could be fulfilled by an accelerometer, enabling the continuous RR monitoring (Inan *et al* 2015). When referring to the respiratory acoustic signal, the RR derived by filtering the SCG/BCG signal can achieve better accuracy than for PPG-derived RR (Haescher *et al* 2015). From the BCG measured by an accelerometer device under a bed mattress, RR and its temporal variability could be derived, with the results in accordance with polysomnography (PSG) (Nurmi *et al* 2016). BCG could be simultaneously extracted with other signals by fiber Bragg grating (FBG), with the maximum error in resultant RR of 1.7 bpm referred to the RR value derived by the respiratory strap (Chen *et al* 2014). RR and HR could be estimated from BCG recorded by the piezoelectric sensor, which is chargeable with GPS and Bluetooth for positioning and data transmission for clinical application (Hermann *et al* 2018). Similar with BCG and SCG, the geophone signals could monitor RR during sleep with the ability of simultaneously monitoring multiple subjects on a bed (Jia *et al* 2017).

2.2.2.5. Algorithms based on OscP and KorS

AM was applied in OscP and KorS for the extraction of respiratory signal (Zheng *et al* 2014), from which RR could be estimated as the peak of power spectral distribution (Di Marco *et al* 2012). Compared with the RR measured by the magnetometer on the chest, the RR estimation was even more accurate under deep breathing (mean \pm SD of error: -0.005 ± 0.053 bpm for OscP-derived RR, -0.010 ± 0.058 bpm for KorS-derived RR) than under normal breathing (0.006 ± 0.066 bpm for OscP-derived RR, 0.044 ± 0.083 bpm for KorS-derived RR). Considering the limited bias, the results suggest that RR estimated from OscP or KorS is a potential for clinical applications. However, under deep breathing, the blood pressure could decrease by 4.8 mmHg, approaching the threshold of 5 mmHg that could lead to incorrect treatment based on OscP and KorS (Chen *et al* 2016a). Moreover, the amplitude of OscP was influenced by the RR value and the measurement cuff pressure (Zheng *et al* 2014), demanding more in-depth investigations.

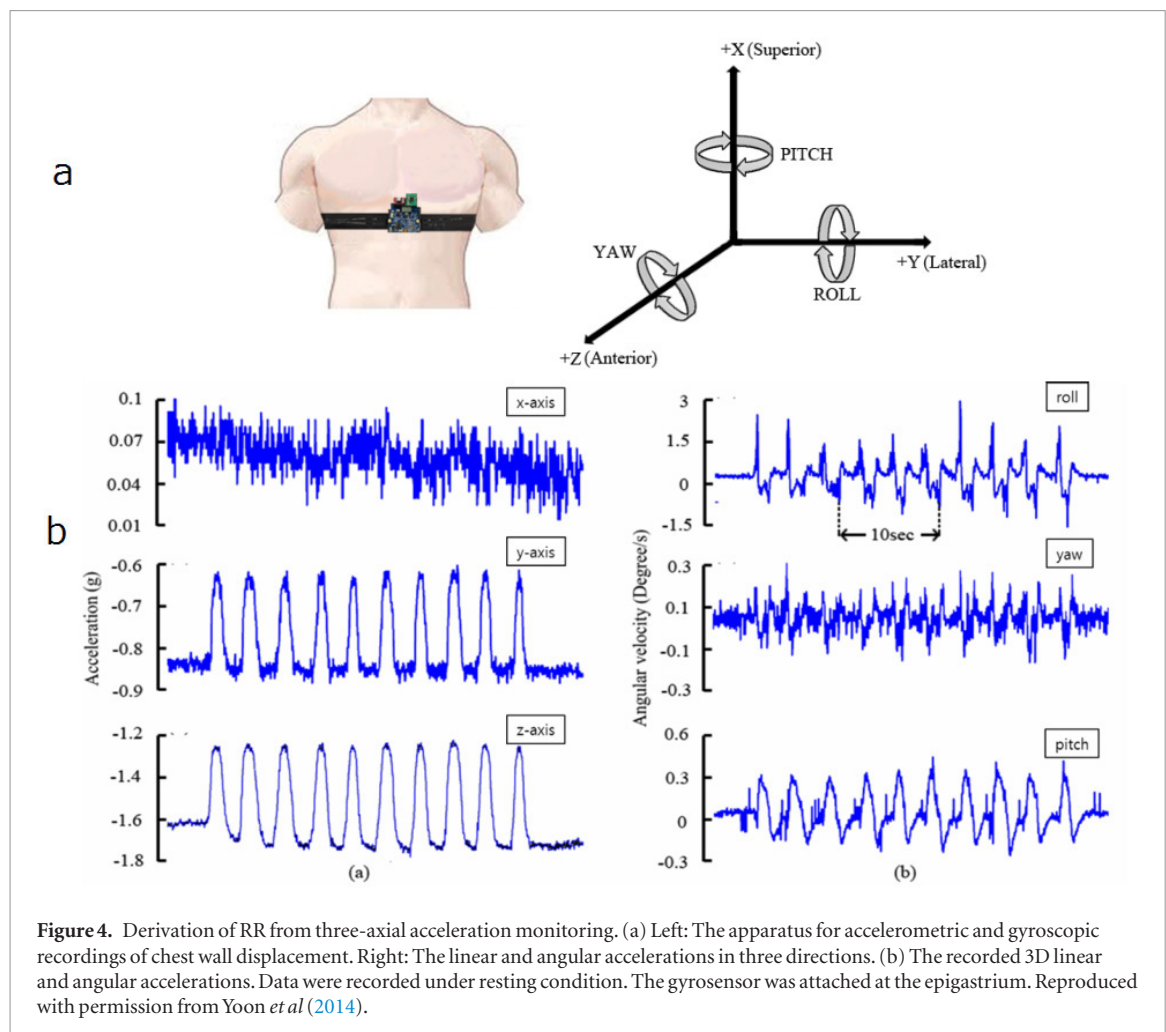
The algorithm based on FM features of OscP and KorS performed better than AM-based algorithms (mean \pm SD of error: 0.002 ± 0.047 bpm for OscP-derived RR, and -0.007 ± 0.056 bpm for KorS-derived RR, referred to the RR derived by a magnetometer on the chest) (Chen *et al* 2016b). However, OscP is sensitive to noise, and methods based on FM (RSA) would not be applicable in subjects with implanted permanent pacemakers, or present recurrent atrial fibrillation, bundle branch blocks, or flat heart rate variability (Damy *et al* 2010).

2.3. Methods based on volume changes and body movement

During inhalation and exhalation, there are periodic volume changes in the thoracic and abdomen areas with movements on the surface. These changes could be detected by accelerometers, gyroscopes, radars and WiFi devices, imaging, and various sensors based on electromagnetic, piezoresistive, piezoelectric, and optical mechanisms. These constitute the majority of the methods that directly measure RR.

2.3.1. Accelerometers and gyroscopes

Accelerometers and gyroscopes can be used to capture signals modulated by respiration when appropriately positioned over the diaphragm. The position and orientation of the accelerometer or gyroscope are changed by chest wall expansion and contraction during respiration. A tri-axial accelerometer or gyroscope provides three measurements of the linear or angular accelerations in three orthogonal directions. The component required for analysis is the direction of the acceleration due to gravity in the accelerometer's coordinate system, which is modulated by respiration (figure 4). To obtain a respiratory signal, firstly a single, time varying, acceleration (linear or angular) vector is derived from the three measurements. Secondly, the rotation angle of the acceleration vector about the time-averaged predominant axis of rotation is calculated. Lastly, the respiratory signal is given by the angular velocity—the rate of change of the rotation angle with respect to time. The predominant axis of rotation could be calculated over an extended time period to reduce the effect of noise, which is of particular importance in mobile monitoring (Bates *et al* 2010). Finally, RR could be extracted from the respiratory signal by the methods such as PCA, as in the ECG- or PPG-based methods. It has been proved that a three-axial



accelerometric system can successfully reconstruct the respiration-induced movement, which is necessary to determine the respiratory rate accurately (Jin *et al* 2009).

Accelerometer-derived RR conformed to the results of polysomnography (PSG) (Nurmi *et al* 2016) and manual observation (Jarchi *et al* 2018), which are the clinically standard methods. By using two juxtaposed accelerometers, the motion artefact could be eliminated from the simultaneous accelerometric signals, with resultant RR in accordance with the results derived by visual counting and spirometry on normal subjects and scoliotic and obese patients under resting and exercising situations (Lapi *et al* 2014). Therefore, the accelerometer has been applied to provide a reference RR value (Liu *et al* 2016, Shirkovskiy *et al* 2017) or reference signal for eliminating motion artefacts in some pilot studies of RR estimation (Sun and Thakor 2016). The accelerometer-derived respiratory signal or RR value could be combined with those derived by other methods such as ECG (Liu *et al* 2013), PPG (Shen *et al* 2017), camera (Hernandez *et al* 2014) and pyro-electric infrared (PIR) sensor (Erden *et al* 2015). Finally, the small size of state-of-art accelerometers enables its versatile application in the smartphones (Camcı *et al* 2017), smartwatch (Trimpop *et al* 2017), mattress-based sleep monitoring (Nurmi *et al* 2016), and head-mounted wearable device (Hernandez *et al* 2014).

A gyroscope could derive more accurate RR estimation (mean \pm SD of the error referred to the value derived by the chest strap: 1.39 ± 2.29 bpm) than the accelerometer (2.26 ± 3.38 bpm) (Hernandez *et al* 2014). However, a gyroscope consumes more energy than an accelerometer (Trimpop *et al* 2017). The combination of an accelerometer and a gyroscope could enhance the accuracy of RR estimation (Shen *et al* 2017). By fusing gyroscopic results by Kalman filtering, the error rate in RR estimation declined from 11.7% of accelerometric results to 7.3% (Yoon *et al* 2014). With a new physiological signal acquisition patch in which the accelerometer and gyroscope were integrated, RR was derived from data fusion with the mean absolute error of 0.11 ± 0.7 bpm (mean \pm SD) and maximum error within 1.6 bpm, in comparison with manually counted RR value (Wang *et al* 2018).

2.3.2. Piezoresistive and piezoelectric pressure sensors

The fluctuations in pressure due to the respiratory effects could change the resistance in piezoresistive sensors and develop electrical potential (charge) in piezoelectric sensors. The piezoresistive and piezoelectric sensors are

potential for wearable and continuous RR monitoring since they could be fabricated into chest straps or clothes (Mahbub *et al* 2017b), and have been applied as the reference for RR monitoring in related studies (Bahmed *et al* 2016, Sifuentes *et al* 2016). Wearable piezoresistive fabric sensors could monitor RR under various moving environments from rapid running to slow walking (Jeong *et al* 2009). Furthermore, as shown in figure 5, the piezoresistive sensor could be applied in the cardiorespiratory sensor system embodied by an automobile safety belt, which enables the real-time monitoring of RR for drivers (Hamdani and Fernando 2015). Clinically, RR monitored by the piezoelectric device achieved relative accordance with both ECG-derived RR (mean \pm SD of the difference: -0.41 ± 1.79 bpm) and RR manually observed by nursing staff (-0.58 ± 2.5 bpm) in 48 post-surgical patients (Lee 2016). As shown in the right column of figure 5, an integrated sensor system of a piezoelectric belt and ECG was used to monitor the respiratory cycle variability for detecting apnea/hypopnea periods (Adnane *et al* 2009).

Recent developments in piezoresistive and piezoelectric sensors enables the mobile and continuous RR monitoring in different situations. With the piezoelectric sensor encapsulated within the sensor patch, the motion artefact, which affects the accuracy of RR monitoring in many chest straps (Atalay *et al* 2015), could be eliminated, enabling the respiratory monitoring in a dynamic walking condition with high fidelity (Lei *et al* 2015). By adding grapheme to the PVDF piezoelectric membrane, the sensibility of the chest strap at body temperature (37°C) could be improved (Hernández-Rivera and Suaste-Gómez 2017). Based on distributed capacitance similar to the piezoelectric sensors, a new elastic displacement transducer could fulfill the wearable respiratory plethysmography besides RR monitoring (Mokhlespour Esfahani *et al* 2013). With a sheet of e-Textile fabric coated with piezoelectric polymer, the underbody pressure distribution was delineated on the high-resolution pressure images. With a robust body parts localization algorithm, respiratory signals extracted from the localized torso area were insensitive to arbitrary extremities movements (Liu *et al* 2015b). A respiratory signal could be derived from the chest movement by the piezoelectric transducer based on PVDF film. After digitalization, the signal was then transmitted by the impulse radio ultra-wideband (IR-UWB) transmitter, fulfilling the mobile RR monitoring at a low energy (Mahbub *et al* 2016). For RR estimation, BCG signal could be measured from the quasi-piezoelectric sensor made of an electroactive polymer material (EMFIT), in which the combination with GPS, Bluetooth and a rechargeable battery made the constant RR monitoring more convenient (Hermann *et al* 2018).

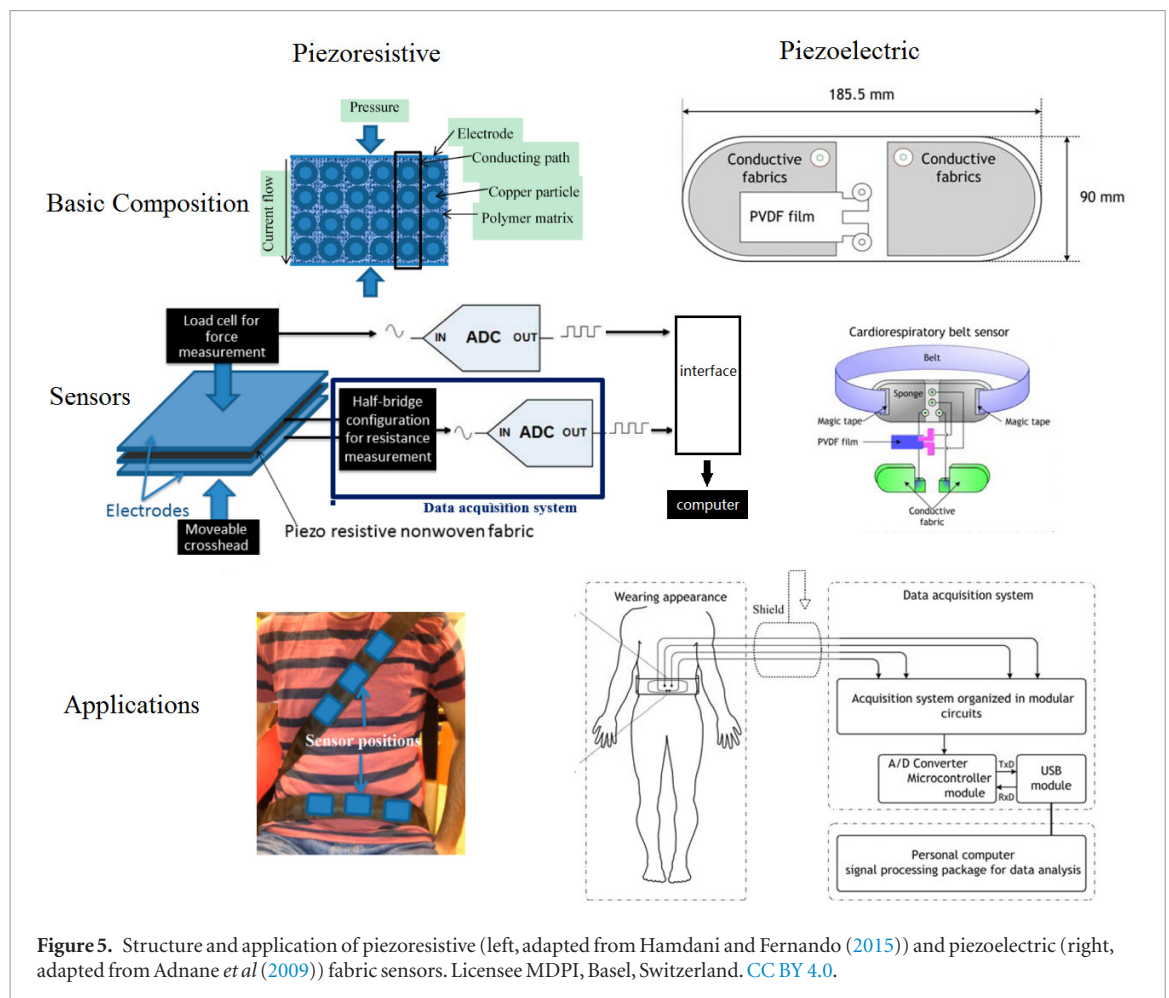
2.3.3. Radio frequency (RF) methods: radar and WiFi

Some RR monitoring systems are based on radio frequency (RF) techniques, which leverage RF signals to capture breathing and heart movements. RF techniques could fulfill the continuous indoor RR monitoring without sensors attached on the human body. The existing techniques can be classified into radar-based and WiFi-based approaches (Huang 2018).

Radar-based RR monitoring has been proposed since the 1970s (Sun and Matsui 2015). Some commonly used radars in RR monitoring include continuous wave (CW) Doppler radar (Chung *et al* 2016), ultra-wideband (UWB) radar (Kocur *et al* 2017), frequency modulated continuous wave (FMCW) radar (Adib *et al* 2015, Van Loon *et al* 2016), and stepped-frequency continuous wave (SFCW) radar (Dang *et al* 2015). Compared with other non-contact RR monitoring methods, such as thermal imaging and video camera imaging, RF methods could provide larger detection areas, with the distance of detection longer than 3 m (Al-Naji *et al* 2017). Physiologically, respiration provides an important radar-based body-detection method since it was the only observable body movement in sleep and coma (Kocur *et al* 2017). Respiration also influences the radar detection of organs and tumor (Li *et al* 2017).

The application background of radar-derived RR has been extended in recent studies. The simultaneous monitoring of multiple subjects could be fulfilled by UWB and SFCW radars (Dang *et al* 2015, Kocur *et al* 2017). By transforming the smartphone into an active sonar device using 18–20 kHz sound waves, the Doppler radar could simultaneously monitor RR on multiple subjects. The apnea detection was then performed on 57 normal subjects and 87 patients, with 0.0023% and 0.0336% positive and negative false rates in detecting sleep apnea events compared with PSG results (Nandakumar *et al* 2015). In a pilot study including eight patients in the post-operative anesthesia care unit (PACU), the FMCW radar derived RR during mechanical and spontaneous ventilations with the errors of -0.12 ± 0.83 bpm and -0.59 ± 2.67 bpm (mean \pm SD, in comparison with the value measured by pneumotachograph during mechanical ventilation and capnometry during spontaneous breathing) (Van Loon *et al* 2016). The radar-based RR monitoring could be integrated with thermal and HR sensors for the portable and real-time screening of infectious patients in public places such as airports (Sun *et al* 2018). A 2.4 GHz DC coupled multi-radar system, which eliminated signal distortions, was applied in detecting different respiration patterns (natural breathing, chest breathing and diaphragmatic breathing), providing a non-contact method for monitoring the physiological and emotional changes (Gu and Li 2015).

The accuracy of radar-based RR monitoring depends on the body position, with a strong influence of body movements (Shamsir *et al* 2018). Within the distance of 8m and in different directions, the wireless RR sensing by the FMCW radar could achieve the accuracy over 97%, compared with the reference RR value measured by a



chest strap. But the measurement is limited to the quasi-static users (e.g. typing, watching TV). This is because signal variations due to full body motion would otherwise overwhelm the small variations due to vital signs (Adib *et al* 2015). The radar-based RR detection is based on sensing the tiny chest wall movements (approximately 1.0–5.0 mm) which are much smaller than the random body movements. With the autocorrelation model, which is good at extracting the periodicity signals submerged in noise, the error in RR estimation by a Doppler radar could be limited to 0.7 ± 1.4 bpm (mean \pm SD, in comparison with the value measured by contact-type respiratory effort belt) in 15 s measurement (Sun and Matsui 2015).

Compared with a radar system, WiFi-based RR sensors are lower in cost and easier to approach (Madsen *et al* 2016). Off-the-shelf WiFi devices could be used to continuously collect the fine-grained wireless received signal strength (RSS) or channel state information (CSI) around a person (figure 6(b)). From the CSI, the rhythmic patterns associated with respiration and could be separated from abrupt changes due to the body movement (Liu *et al* 2016). RR monitoring based on RSS could estimate different RRs with the error less than 1 bpm in paced breathing (Abdelnasser *et al* 2015). CSI could provide better RR estimation compared with the RSS which would be affected by abnormal breathing. In WiFi-based RR monitoring, the user location and body orientation influence the quality of CSI signals and hence affect the accuracy of RR estimation (Wang *et al* 2016). The WiFi-derived RR showed 88.8% measurement accuracy compared with ventilator capnography (Madsen *et al* 2016). In a WiFi-based respiratory monitoring lasting 200 min at a distance of 2.5 m, the error in respiratory phase difference was 0.337 s and the average accuracy in RR is 89.9%, compared with the banded respiratory monitoring device, with the accuracy of 93.2% in detecting sleep apnea (Bao *et al* 2017). Similar with radar-based methods, WiFi-based RR monitoring could simultaneously measure multiple subjects (Abdelnasser *et al* 2015), and is a promising method for sleep monitoring (Liu *et al* 2015a), especially for patients and the elderly (Bao *et al* 2017).

2.3.4. Electromagnetic sensors: EIP, RIP, EIT and others

In clinical research, conventional non-invasive monitoring of respiration rate is performed by electrical impedance pneumography (EIP) or impedance pneumography (IP). Respiratory inductive plethysmography (RIP) and electrical impedance tomography (EIT) are two monitoring techniques that have been used to assess lung volume noninvasively. RR could also be derived by other electromagnetic sensors that measure the respiratory motion of the chest.

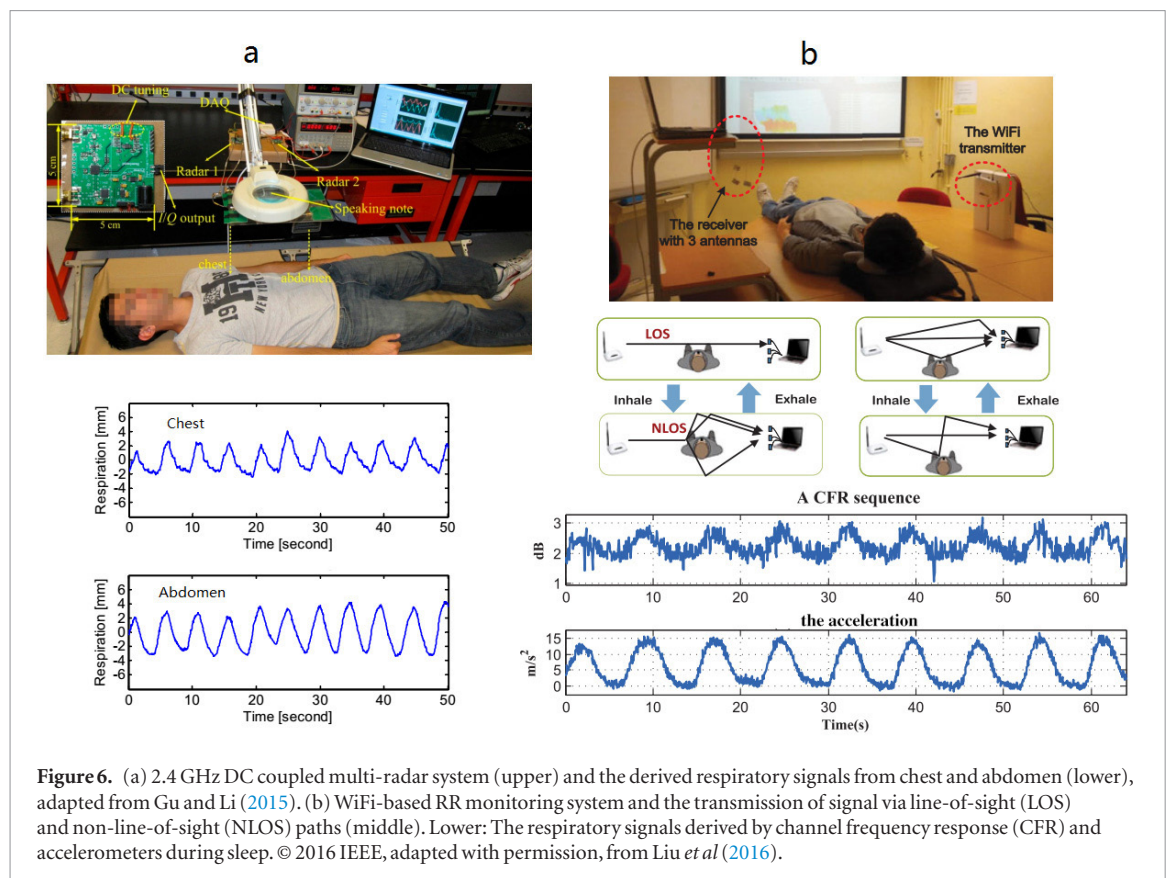


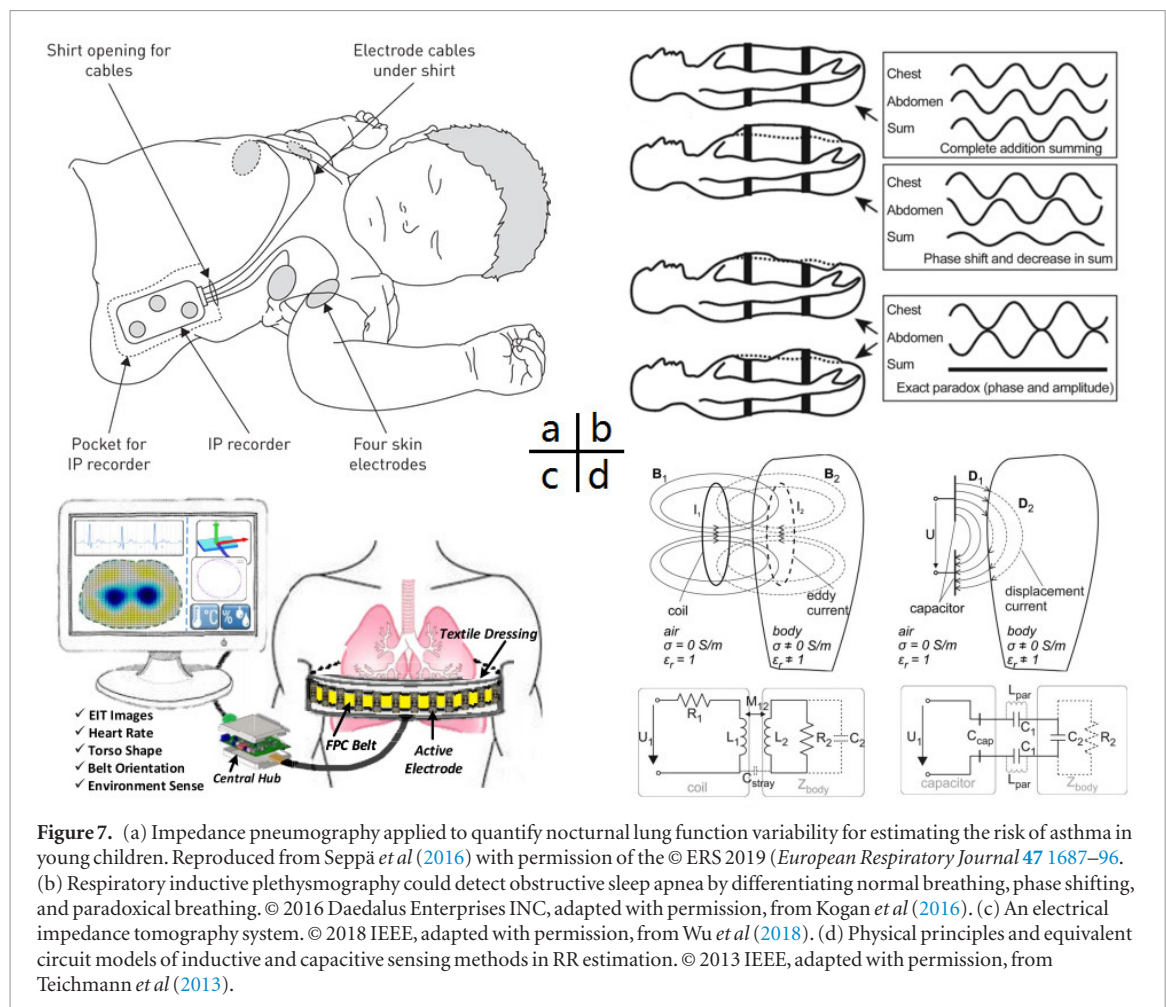
Figure 6. (a) 2.4 GHz DC coupled multi-radar system (upper) and the derived respiratory signals from chest and abdomen (lower), adapted from Gu and Li (2015). (b) WiFi-based RR monitoring system and the transmission of signal via line-of-sight (LOS) and non-line-of-sight (NLOS) paths (middle). Lower: The respiratory signals derived by channel frequency response (CFR) and accelerometers during sleep. © 2016 IEEE, adapted with permission, from Liu *et al* (2016).

EIP (or IP) measures the impedance change caused by the respiration cycle between two electrodes placed on the chest, with the injection of a low-amplitude high-frequency current into the thorax. EIP is widely used in long-term monitoring of respiration during sleep in adults and young children (Seppä *et al* 2016), and has been applied as the reference of RR in studies on ECG- and PPG-based RR measurement (Orphanidou 2017). However, EIP is susceptible to motion and posture changes of the subject and therefore prone to erroneous estimation (Jarchi *et al* 2018). Eight algorithms for deriving RR from EIP signals were compared on 15 subjects (10 males + 5 females) in three conditions: standing, walking in 3 km h^{-1} , and walking in 6 km h^{-1} . The algorithms were three autoregressive (AR) modeling approaches, fast Fourier transform (FFT), autocorrelation, peak detection and two counting algorithms. It was found that the advanced counting method was the most promising approach for EIP-based RR estimation, with the concordance correlation coefficients of 0.96, 0.90 and 0.97 for standing, walking in 3 km h^{-1} , and walking in 6 km h^{-1} , compared with the reference flow thermography (FTG) results (Jeyhani *et al* 2017). Besides algorithmic improvements, the data fusion with accelerometers and gyroscopes could also improve the accuracy of EIP-based RR estimation, with the error of $0.7 \pm 1.0 \text{ bpm}$ and $3.0 \pm 2.6 \text{ bpm}$ (mean \pm SD, compared with the capnography RR results) under static and running states (Shen *et al* 2017).

Recently, there are ECG front-end modules embedding an impedance channel for respiration measurement (Jekova *et al* 2014, Abtahi *et al* 2015). Such modules could simultaneously record ECG and respiration signal without the need for extraction of the respiration signal from the ECG signal. The calculation of RR in these modules are based on thoracic impedance instead of respiratory modulations.

RIP employs two copper wires: the transducer is placed around the rib cage around the abdomen with the other on the chest (figure 7(b)). During the respiration cycle, volumetric differences occur and this causes self-induction of the two wires. On the screen of the oscillator, the change in frequency is shown as a digital respiration waveform. Clinically, with post hoc analysis based on age-matched reference values, RIP could estimate many indices besides RR such as phase angle, laboured breathing index, and percent of rib cage contribution to breathing (Balasubramaniam *et al* 2018). RIP could estimate tidal volume within $\pm 10\%$ error compared with the reference flowmeter in 93.9% of the total of 11 437 breaths, with the device power less than 23.1 mW (Zhang *et al* 2012). Due to its ability to measure the volumetric changes, RIP could be used to detect obstructive sleep apnea by analyzing RR and the phase changes during respiration (Kogan *et al* 2016). For respiratory monitoring in pediatric patients treated with patient-controlled analgesia, RIP is more appropriate than capnography due to its long-term tolerability (Miller *et al* 2015).

EIT is a radiation-free functional imaging modality invented over 30 years ago. During an EIT examination, very small alternating electrical currents are applied through pairs of electrodes while the resulting voltages are measured on the remaining electrodes. A general EIT measurement process includes: (1) execution of EIT



measurements, (2) generation of raw EIT images, (3) EIT waveforms and regions-of-interest (ROI), (4) functional EIT images, and (5) EIT measures (figure 7(c)) (Frerichs *et al* 2016). As RIP, EIT could also provide tidal volume besides RR (Wolf and Arnold 2005). A wearable EIT system could fulfill the simultaneous measurement of HR, RR, incubator temperature and humidity for monitoring preterm infants, with the belt orientation and patient torso detection aiding EIT model selection for enhanced image reconstruction (Wu *et al* 2018).

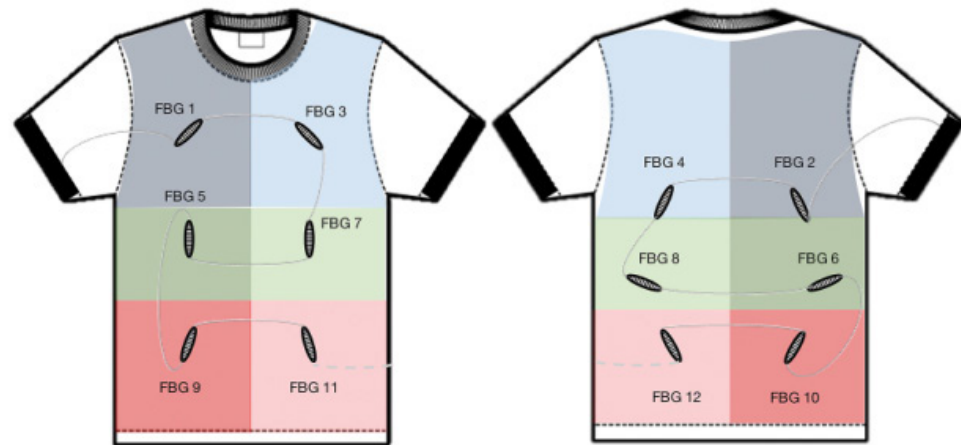
Besides EIP, RIP and EIT, other electromagnetic sensors are emerging for RR monitoring, based on magnetic flux density (Oh *et al* 2018), magnetic induction (Teichmann *et al* 2015), magnetic eddy current induction and displacement current induction (Teichmann *et al* 2013). By measuring thoracic impedance during respiration, RR was measured in 30 patients of drug or alcoholic poisoning with the error of 0.3 ± 5.5 bpm (mean \pm SD, compared with gold standard capnometry results) (Guechi *et al* 2015). Noticeably, a capacitive electrical field sensor array placed under a bed mattress derived the unobtrusive and contactless RR measurement with the accuracy of 0.0 ± 0.41 bpm (mean \pm SD, compared with flowmeter results) (Wartzek *et al* 2011). Although mostly at the experimental stage, these innovative devices are promising in consideration of their accuracy.

2.3.5. Optical sensors

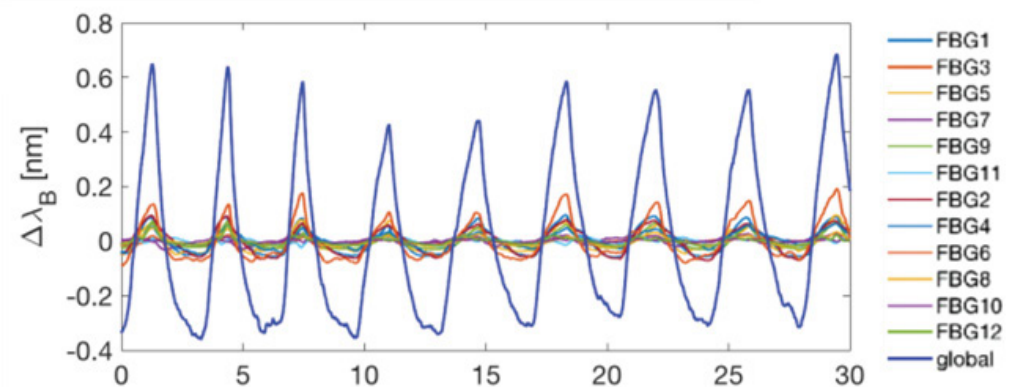
The very small dimensions of optical fibers allow them to be encapsulated inside very thin catheters and injection needles, thereby enabling localized monitoring of thoracic movement to derive RR (Fajkus *et al* 2017). Macrobend (Koyama *et al* 2018, Purnamaningsih *et al* 2018, Witt *et al* 2012) and microbend (Chen *et al* 2013, 2014, Yang *et al* 2015b) optic fibers are adopted to transform the movements to the fluctuations in the intensity of optic signals. The fiber Bragg grating (FBG) is widely used in RR monitoring. Besides RR, FBG could provide multiple physiologic parameters such as tidal volume (Massaroni *et al* 2018), heart rate (Fajkus *et al* 2017), and heart sound (Ogawa *et al* 2018).

FBG RR sensors showed considerable accuracy. Consisting of 12 FBG sensors on thoracic and abdomen areas and corresponding areas on the back, a wearable FBG array achieved RR values comparable with those measured by a six-camera motion capture system (mean \pm SD of error: -0.02 ± 1.04 bpm)(figure 8). The inspiratory and expiratory phases, breathing duration and tidal volume also indicated accordance with the reference values (Massaroni *et al* 2018).

a



b



c

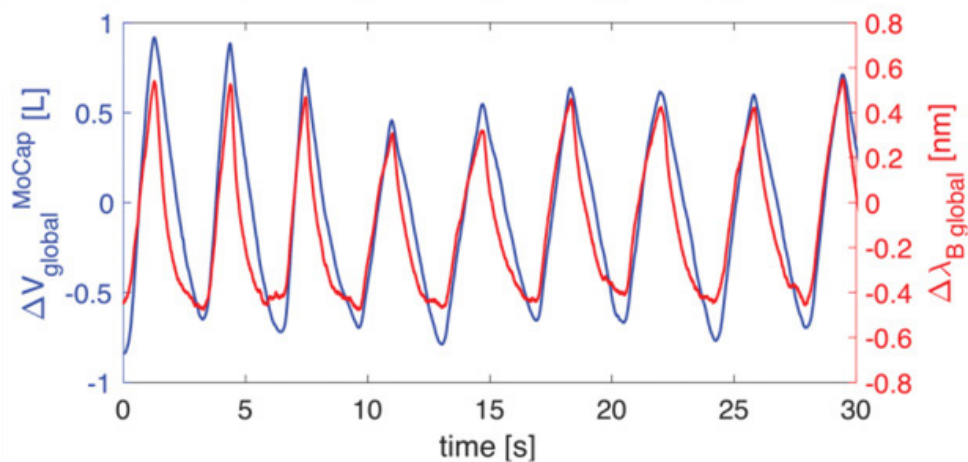
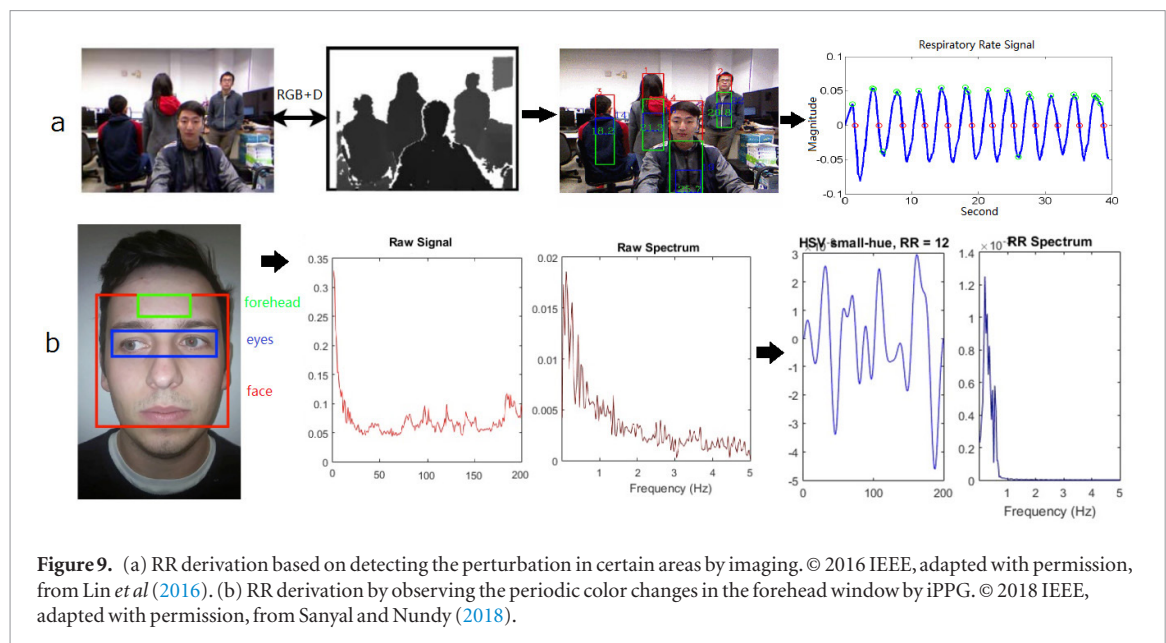


Figure 8. (a) The FBG sensor array. (b) The global respiratory signal (the length of wavelength) derived from the 12 FBG sensors. (c) The accordance of respiratory signals derived by FBG and a motion capture system. Massaroni *et al* 2018 John Wiley & Sons. © 2018 Wiley-VCH Verlag GmbH & Co. KGaA, Weinheim.

Referring to the six-camera motion capture system, the application of a male-fit wearable FBG array on women derived correct RR values (mean \pm SD of error: 0.014 ± 1.218 bpm), with significant errors in tidal volume (Presti *et al* 2018).

Optical fiber sensors have many advantages such as electromagnetic immunity, chemically inert nature, intrinsically safe modes of operation and light weight (Yang *et al* 2015b). Especially, optic sensors could be applied in MRI examinations for which metallic sensors are inapplicable (Chen *et al* 2014). In biomedical applications, plastic optical fibers (POFs) could avoid fiber break, which is a limitation of glass optical fiber, therefore are more biocompatible (Chen *et al* 2013). The macrobend optical fibers could measure RR under different physiological conditions including standing, walking, running, and sleeping (Purnamaningsih *et al* 2018). Additionally, fiber-optic sensors such as FBG could be fabricated into chest straps (Fajkus *et al* 2016) and T-shirts (Massaroni *et al* 2018, Presti *et al* 2018). The results could be transmitted to computers by Bluetooth for signal analysis (Yang *et al* 2015b). Therefore, optical fiber sensors are promising for wearable and portable RR monitoring. However, the optical sensors are still at the experimental stage with further applications limited by the high cost (Witt *et al* 2012). More low-cost optical fibers and validations are needed in further studies.



2.3.6. Imaging and iPPG

RR could be derived without body contact by detecting and analyzing the body movement with camera-based monitoring systems. Combining the imaging and PPG techniques, the imaging PPG (iPPG), also known as video PPG (vPPG) or PPG imaging (PPGI) is another promising method that extracts RR from the periodic fluctuations of blood volume.

In figure 9(a), an image covering the subject's head area was firstly captured with depth data and then the upper body area was automatically selected. After Gaussian filtering to smooth the original signal, the respiratory motion in the salient area to the head enclosed by a green bounding box was modeled by the vertical variation of optical flow derived by a Jacobi solver. This method was primarily validated on 41 video clips recorded from nine subjects in a sitting position, with the error of -0.32 ± 0.82 bpm in comparison with the RR values derived by the chest strap (Lin *et al* 2016). Based on a low-cost 'off-the-shelf' game console 3D time-of-flight camera, RR was detected accurately, with the errors in vital capacity within $\pm 1\%$ in comparison with spirometry (Sharp *et al* 2017).

Imaging-based RR estimation could be performed on adults and young children (Rehouma *et al* 2017) in different positions (Reyes *et al* 2017, Braun *et al* 2018) with different cameras. A major superiority of the imaging-based method is that RR could be estimated in a wide range, especially in the high frequency range, from both the chest and abdomen (Nam *et al* 2016a). The respiratory motion could be extracted from other locations such as the skeletal joints (Marques *et al* 2018). Using a colour or near-infrared (NIR) camera under illuminated and dark conditions respectively, RR was measured on 16 healthy adults. The overall error was 0.2 ± 1.17 bpm (mean \pm SD, compared with the thoracic strain gauge belt) with limited difference between color and NIR cameras (color: 0.25 ± 0.97 bpm, NIR: 0.24 ± 1.03 bpm). This approach had low computational complexity, therefore facilitating a real-time implementation (Braun *et al* 2018). Using the camera on an Android smartphone, RR was measured with the errors of -0.024 ± 0.421 bpm (mean \pm SD, compared with a spirometer reference), indicating the feasibility of developing an inexpensive and portable breathing monitor based on smartphones (Reyes *et al* 2017).

The state-of-art smartphones are able to measure PPG signals by contact and non-contact methods from the finger and forehead respectively (Papon *et al* 2015). In iPPG methods, RGB videos of the forehead were analyzed to derive the periodic signals of blood flow, from which RR could be derived as in PPG-based methods using similar algorithms such as FM (Mirmohamadsadeghi *et al* 2016). The iPPG signal is often derived from variations in the intensity of the green channel, while other imaging properties such as the variations in color of reflected light were also applied in RR estimation (Sanyal and Nundy 2018). In different distances and positions, the SFCW radar and iPPG indicated a comparable ability in detecting the RR of human subjects (Ren *et al* 2017). The iPPG signal is substantially noisier than the equivalent PPG signal from pulse oximeters (Pimentel *et al* 2017). Compared with PPG-based RR monitoring, the contact-free nature of iPPG allows the monitoring of sensitive skin areas like premature infant's skin, ulcers, or burn wounds (Bruser *et al* 2015).

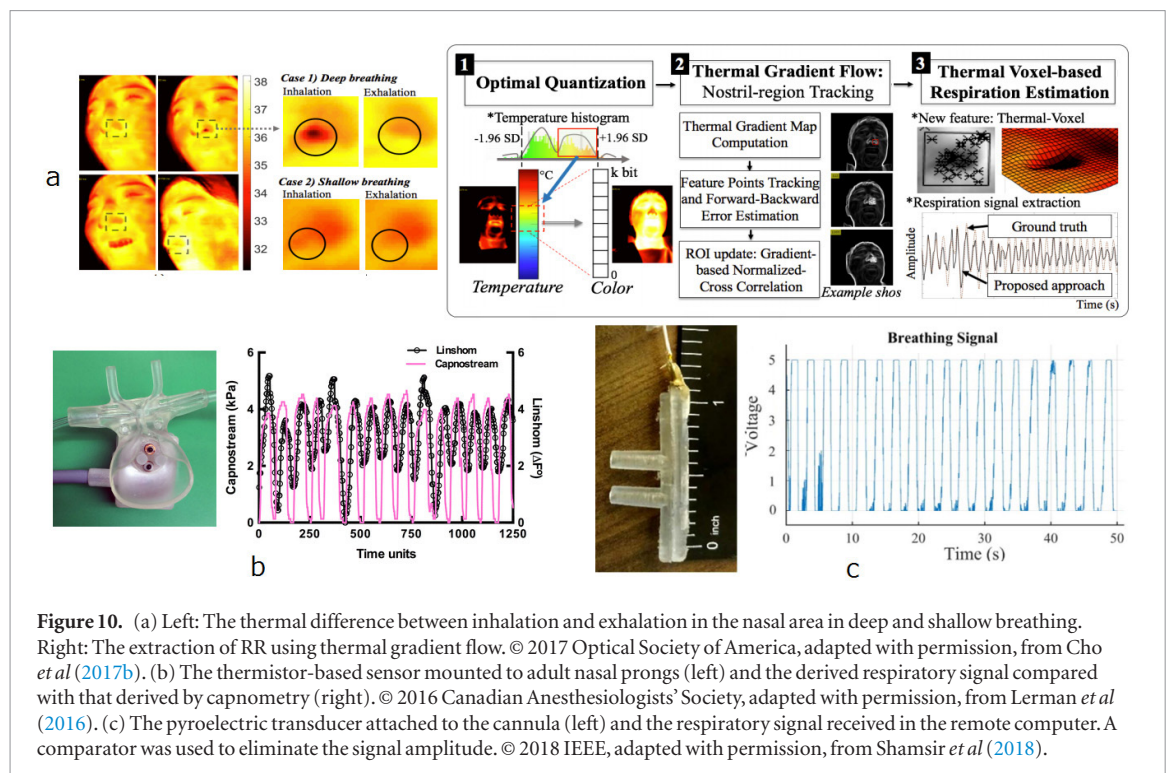


Figure 10. (a) Left: The thermal difference between inhalation and exhalation in the nasal area in deep and shallow breathing. Right: The extraction of RR using thermal gradient flow. © 2017 Optical Society of America, adapted with permission, from Cho *et al* (2017b). (b) The thermistor-based sensor mounted to adult nasal prongs (left) and the derived respiratory signal compared with that derived by capnometry (right). © 2016 Canadian Anesthesiologists' Society, adapted with permission, from Lerman *et al* (2016). (c) The pyroelectric transducer attached to the cannula (left) and the respiratory signal received in the remote computer. A comparator was used to eliminate the signal amplitude. © 2018 IEEE, adapted with permission, from Shamsir *et al* (2018).

2.4. Methods based on airflow changes

The respiratory airflow causes various effects around the nasal area: the periodic fluctuations in temperature, humidity, the density of carbon dioxide, and the sounds. RR could be derived by the sensors based on these effects.

2.4.1. Thermal imaging, thermistors, and pyroelectric transducers

Generally, RR extraction from thermal imaging depends on the fluctuation of signal intensity (figure 10(a), left). With the highly portable FLIR ONE thermal camera device, which provides thermal and visual images by turns, the region-of-interest (ROI) was firstly located within the face and nose region. The histogram equalization and Kanade–Lucas–Tomasi (KLT) methods were then employed to enhance the image and track the subject to prevent the ROI location error. With Hilbert–Huang transform, the accuracy of RR extraction was improved (-0.71 ± 1.98 bpm, Mean \pm SD of error, referred to the LabQuset2 gas pressure sensor results) compared with FFT (-2.25 ± 3.05 bpm) (Chen and Lai 2017). With the breathing sorption indicator (BSI) mask on which the nasal airflow blows, due to the high (approximately 2.3 kJ g^{-1}) specific heat of water evaporation, the thermal changes could be amplified on the mask (10°C , over 100 times compared with that derived directly from nasal airflow), providing the possibility of remote thermal imaging for RR estimation (Vainer 2018).

Clinically, the RR extracted from the infrared thermograph conformed to the results derived from body surface ECG (1.75 ± 2.29 bpm, mean \pm SD of error) (Hochhausen *et al* 2018). Compared with the ECG-based method, the thermal imaging is less influenced by the motion artifact, but it highly depends on the thermal scene of the subject. Large head movements could also deteriorate the accuracy of RR estimation based on thermal imaging (Alkali *et al* 2017). Based on the thermal imaging derived by the mobile thermal camera (FLIR One for Android), which detects electromagnetic waves in the spectral range of $8\text{--}14 \mu\text{m}$, a thermal gradient map-based visual tracking technique was proposed to enhance the RR extraction in scenes with high thermal dynamic ranges and body movements. On the dataset derived from eight healthy subjects with unconstrained respiration in fully mobile context and varying thermal dynamic range scenes, the gradient-based RR showed better accuracy (-0.14 ± 2.45 bpm, mean \pm SD of error, referred to chest-belt respiration sensor) than the traditional method (-0.19 ± 2.59 bpm) (figure 10(a)) (Cho *et al* 2017b).

The accuracy of RR estimation depends on the quality of thermal imaging (Hu *et al* 2018). The major limitations of thermal imaging methods include long processing time (Daw *et al* 2016) and high cost (Bruser *et al* 2015). However, it is a non-contact method, and could be applied for sleep monitoring where other imaging methods with illumination are unavailable (Daw *et al* 2016).

During inhale and exhale activity, the changes of airflow temperature near the nose and mouth could be detected from fluctuations in the resistance of a thermistor, providing the estimation of RR. Compared with other RR measurement systems, the thermistor is a low-cost one with high precision for the detection of apnea (Das *et al* 2017), and is therefore widely adopted as the clinical standard for apnea detection (Gray and Barnes

2017). In the traditional circuit, the analog-to-digital convert could cause self-heating, which might deteriorate the RR estimation. With the time-modulated respiratory signal directly digitized with the microcontroller, it was not necessary to supply any voltage or current to the thermistor, the self-heating was therefore avoided. In 27 subjects, the results were in good accordance with the results derived by a piezoelectric sensor on the chest belt (mean \pm SD of error: 0.017 ± 0.155 bpm) (Sifuentes *et al* 2016). To eliminate the effects of environmental thermal fluctuations, in a temperature-based noninvasive instrument of RR monitoring, two rapid responding medical-grade thermistors were respectively in close proximity to the mouth/nose and remote to the airway as a reference. The measured RR conformed well to the capnometry results (mean \pm SD of error: -0.17 ± 1.01 bpm) in the pilot study on three subjects, but needs further validation (Lerman *et al* 2016). Due to its low cost, the thermistor is applicable for the portable monitoring of RR especially in low-resource settings (Turnbull *et al* 2018).

Besides the thermistors, pyroelectric transducers, which transduce temperature variations into an electrical signal, have also been applied in RR monitoring. The acquired signal could be processed through an electronic circuit fabricated using a standard CMOS process, thus obtaining an electronic device with low power consumption (Pullano *et al* 2017). Based on pyroelectric transducers, RR monitoring systems could be low-power (Mahbub *et al* 2015) or self-powered (Mahbub *et al* 2017a). Polyvinylidene-fluoride (PVDF), which has both piezoelectric and pyroelectric properties, is widely adopted in pyroelectric RR monitoring systems (Pullano *et al* 2016). Besides the nasal apparatus, the pyroelectric nanogenerator could fulfill wearable and portable RR monitoring (Xue *et al* 2017). As a promising method, currently the pyroelectric sensors for RR monitoring are generally on the experimental stage, in need of the large-scale validation on subjects.

2.4.2. Acoustic sensors

Respiratory airflow could be acoustically measured from tracheal and nasal areas or ear canal by contact and noncontact methods (Al-Khalidi *et al* 2011). Acoustic sensors could be capsulated in different apparatus and applied for RR monitoring in different situations. Acoustic methods could achieve high accuracy in RR estimation. During intravenous sedation in dental procedures, there was no significant difference ($p > 0.05$) between the RR values derived by electrical stethoscopes and capnography (Morimoto *et al* 2018). For a total of 137 199 paired RR values measured by acoustic and capnography methods, the bias, standard deviation, and limits of agreement of respiration rate from acoustic monitoring versus capnography were 0.2 ± 2.3 bpm and -4.2 to 4.7 bpm, indicating good overall agreement of the two methods (Tanaka *et al* 2014). Based on a phonocardiogram (PCG) and a capacitor microphone near the mouth, a wireless acoustic sensor derived RR estimation comparable to the results of the chest strap (mean \pm SD of error: 0.1 ± 0.63 bpm) (Abbasi-Kesbi *et al* 2018). For the RR monitoring after extubation in ICU patients, referred to as capnometry, the acoustic sensor (mean \pm SD of error: 0.3 ± 2.12 bpm) achieved comparable accuracy with thoracic impedance (0 ± 3.24 bpm) (Autet *et al* 2014). In obese patients recovering from general anaesthesia, the accuracy of RR estimation by acoustic method (mean \pm SD of error: -0.3 ± 1.81 bpm, referred to capnometry) was also comparable to and even better than the results derived by the impedance method (-0.6 ± 2.70 bpm) (Frasca *et al* 2015). In some studies, the RR value measured by the acoustic method was used as the reference value (Haescher *et al* 2015, Turnbull *et al* 2018).

A clinical study indicated that adding continuous acoustic RR monitoring to a pulse oximetry-based surveillance system may not significantly improve patient deterioration detection (McGrath *et al* 2017). In clinical applications such as dental scaling, the accuracy of acoustic RR estimation is significantly influenced by the noise ($p < 0.001$) (Kim *et al* 2018), especially when RR value is low (Yabuki *et al* 2018). Despite these limitations, acoustic methods could measure RR values as high as 90 bpm (Nam *et al* 2016b), which is difficult for many other methods, and is available in various apparatus from the hearing protection devices (figure 11(a)) to smartphones (figure 11(b)) (Reyes *et al* 2016, Martin and Voix 2017). Therefore, the acoustic method is promising in fulfilling accurate and portable RR monitoring.

2.4.3. Humidity sensors and capnometry

The material composition of airflow differs between inhalation and exhalation. The exhaled air is more humid with a higher ratio of carbon dioxide. Various humidity sensors and capnometry apparatus therefore have been developed to measure RR.

Various humidity sensors have been developed based on humidity-sensitive materials such as graphene oxide (Caccami *et al* 2017), silica nanoparticles (SiO₂ NPs) (Kano *et al* 2018), quartz crystal microbalance (QCM) (Selyanchyn *et al* 2015), coronene tetracarboxylate (CS)-dodecyl methyl viologen derivative (DMV) nanofibres (Mogera *et al* 2014), and synthetic redox conducting supramolecular ionic material (SIM) (Yan *et al* 2016). Other methods in humidity-based RR monitoring include digitally printing graphite ink (Güder *et al* 2016), a CMOS-MEMS device (Lai *et al* 2014), and Trichel pulses (TPs) measured by a field ionization sensor consisting of a needle electrode and a plate electrode (Deng *et al* 2014).

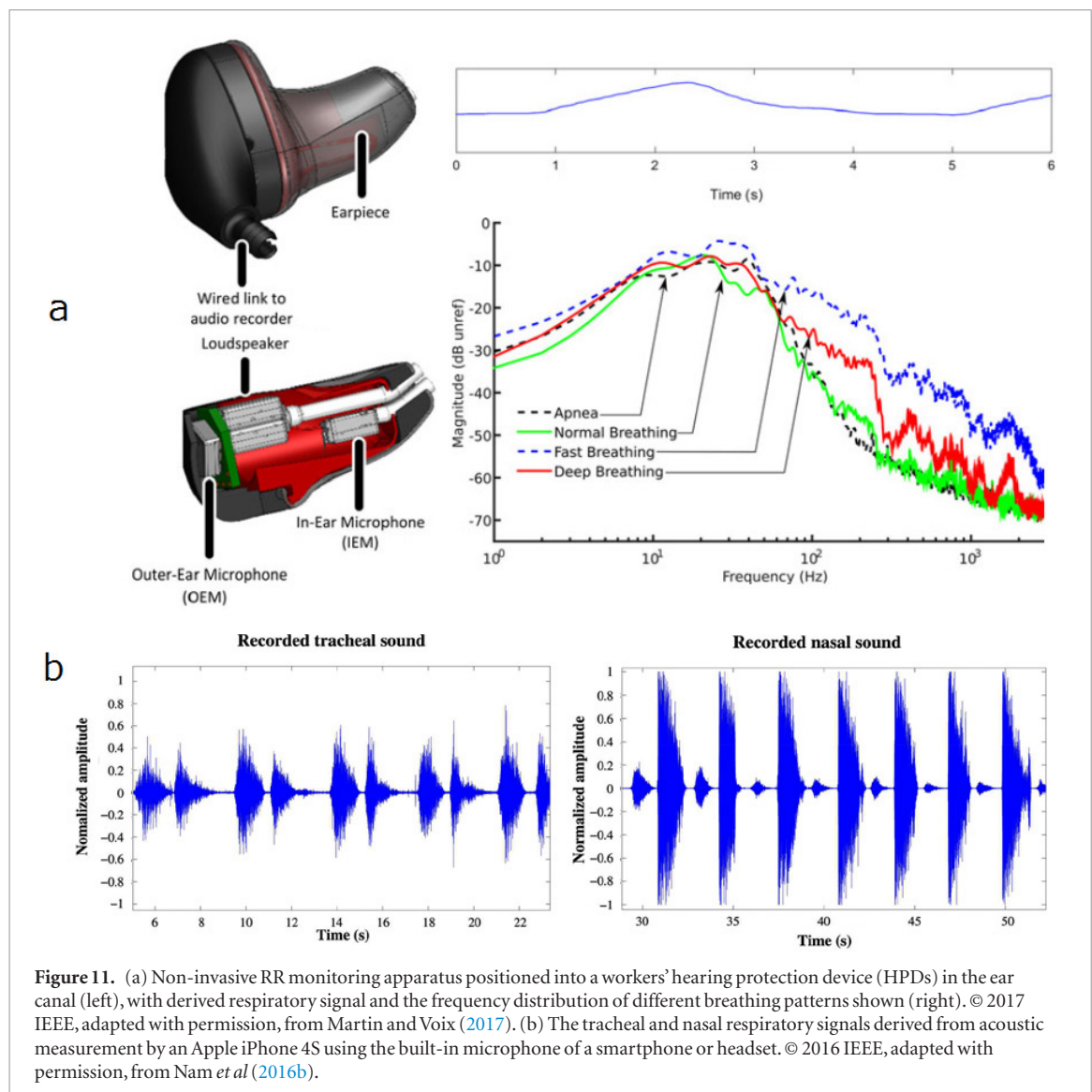


Figure 11. (a) Non-invasive RR monitoring apparatus positioned into a workers' hearing protection device (HPDs) in the ear canal (left), with derived respiratory signal and the frequency distribution of different breathing patterns shown (right). © 2017 IEEE, adapted with permission, from Martin and Voix (2017). (b) The tracheal and nasal respiratory signals derived from acoustic measurement by an Apple iPhone 4S using the built-in microphone of a smartphone or headset. © 2016 IEEE, adapted with permission, from Nam *et al* (2016b).

The humidity-based sensors are promising. Firstly, they could fulfill real-time RR monitoring, especially for rapid respiration ($RR > 60$ bpm) (Mogera *et al* 2014, Kano *et al* 2018). The response time to respiratory humidity changes could be less than 40 ms (Lai *et al* 2014, Mogera *et al* 2014, Yan *et al* 2016). Secondly, the humidity sensors could be fabricated into films and attached to masks (Güder *et al* 2016, Caccami *et al* 2017), with the results shown on smartphones, enabling the wearable and portable RR sensing (figure 12(a)). The humidity changes decrease with the distance from the airflow outlets. Therefore, distance is a major limitation of current humidity-based RR sensors, which contact the skin or are at a near distance, such as 10 cm, from the nostril or mouth (Kano *et al* 2018). Additionally, most of the humidity-based RR sensors were at the experimental stage. The validations were performed on limited human subjects (Mogera *et al* 2014) or rats (Yan *et al* 2016). Further large-scale validations on human subjects and the comparison with other existing sensors are needed.

Capnometry has been established as one of the clinical standards for respiratory monitoring. As mentioned, the RR results derived by capnometry were applied as the gold standard in many studies (Autet *et al* 2014, Frasca *et al* 2015, Bergese *et al* 2017). Compared with PPG and acoustic results, the capnogram demonstrated better ability to distinguish between different respiratory rates when the RR value is low (Ermer *et al* 2017). Despite its accuracy, a major limitation of traditional capnometry is its inconvenience for which many patients in the general care floor removed the nasal cannula due to physical annoyance (Addison *et al* 2015). Capnometry via a nasal cannula is difficult to perform on extubated patients after surgery with high nasal airway resistance (Zhang *et al* 2017). Recently, a pyroelectric (Yang *et al* 2015a) and infrared absorption sensor, which measure both main and side streams of respiratory airflow (Degner *et al* 2018), have been applied in capnometry (figure 12(b)). Clinically, the capnometry-derived RR indicated limited ability to provide warning signs for a hypoxaemic event during the sedation procedure (Touw *et al* 2017). In some cases, new acoustic sensors showed better accuracy than capnometry in monitoring RR during anesthesia care (Tanaka *et al* 2014, Morimoto *et al* 2018). Therefore, more convenient capnometry devices, and higher accuracy in capnometry-derived RR during anesthesia, are still needed in further investigations.

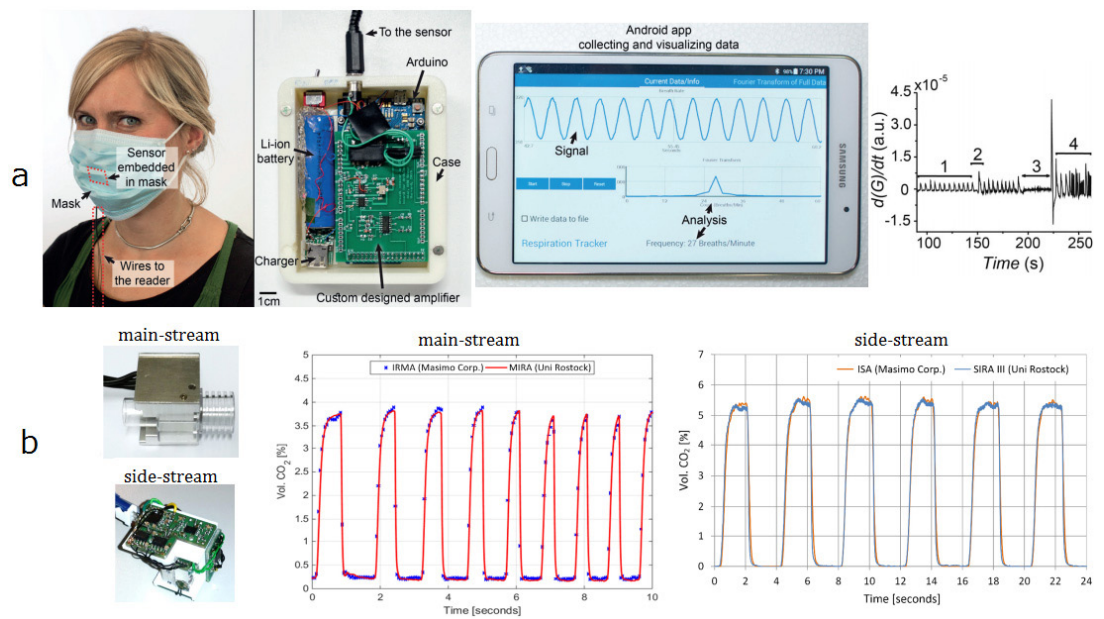


Figure 12. (a) The humidity sensor on the mask and its structure (left), the derived respiratory signal on the Android smartphone (middle), when 1. breathing normally, 2. taking a deep breath, 3. paused and, and 4. random breathing (right). © 2016 John Wiley & Sons, adapted with permission, from Güder *et al* (2016). (b) The capnometry devices, which measure the main-stream and side-stream of the respiratory airflow based on the optical measurement of CO₂ absorption bands in the mid-infrared (MIR), and the derived respiratory signals. © 2018 IEEE, adapted with permission, from Degner *et al* (2018).

Table 2. The summarization of the new methods for RR measurement.

Methods	Wearable	Non-contact	No additional devices	Low cost	Multiple subjects
Respiratory modulation					
ECG	✓		✓		
PPG	✓		✓		
BCG and SCG	✓		✓		
OscP and KorS			✓		
Accelerometer and gyroscope	✓				
Piezoresistive and piezoelectric sensors	✓				
Radar		✓			✓
WiFi		✓		✓	✓
Electromagnetic sensors	✓				
Optical sensors	✓				
Imaging and iPPG		✓			✓
Thermal imaging		✓			
Thermistor	✓			✓	
Pyroelectric transducer	✓				
Acoustic sensors	✓				
Humidity sensors	✓				
Capnometry	✓				

3. Discussion and conclusion

In life-threatening conditions, RR can significantly change in just a few minutes. To provide immediate rescue, continuous monitoring of respiratory activity should therefore be mandatory in high-risk clinical situations such as acute myocardial infarction, short MI, and perennial unexplainable breathing stop, where simple and inexpensive RR monitoring is in need. The monitoring of RR is significant not only in hospital routines, but also in everyday tasks of common people to get an overview of their health. Convenient and accurate RR monitoring is therefore an important issue.

The major methods in RR monitoring have been reviewed according to their technical basis. In this part, their advantages and limitations will be discussed to disclose some future direction, as summarized in table 2.

3.1. Summary of current methods

In each kind of method, we could find some highly accurate RR monitoring results. However, the accuracy depends on different conditions. The methods based on other physiological signals could fulfill the simultaneous monitoring of multiple vital signs, and decrease the cost of RR monitoring. However, the accuracy of estimated RR depends on the quality of the original signal and the algorithm. The fusion of FM, AM and BW does not always obviously enhance the accuracy (Birrenkott *et al* 2018). The methods based on respiratory movements are suitable for wearable (optical, piezoelectric, and electromagnetic sensors) and wireless (radar, WiFi, and imaging methods) monitoring of RR. The body motion, environmental noises, and distance would significantly influence the accuracy. Generally, the methods based on direct measurement of airflow could achieve high accuracy in different motion status. Some of the airflow-based sensors are attached to the skin (FBG sensor, tracheal acoustic sensors) or the nasal areas (thermistors, pyroelectric sensor, capnometry). Some others could fulfill the non-contact RR monitoring (thermal imaging, distant acoustic sensors) but the accuracy depends highly on the environment.

All these methods could derive continuous respiratory waveforms with RR. Breath-to-breath RR variations were only investigated in some clinical studies (Adnane *et al* 2009, Nurmi *et al* 2016, Seppä *et al* 2016). In many methods, such as the methods based on respiratory modulation, the acoustic sensors, only RR value could be directly derived. The respiratory waveform are derived from breath-to-breath results by curve-fitting. For methods based on thermal imaging, capnometry, and humidity sensors, the amplitude of the respiratory curve is non-linearly related to respiratory airflow, with possible delay in phase.

This review focused on the state-of-art techniques in RR monitoring. Therefore, the majority of the reviewed methods were at the experimental stage and in need of further validation. Traditional methods, such as the EIP, capnometry, and piezoelectric respiratory straps have been well validated and applied as clinical references. Many methods included some primary validation in which the estimated RR was compared with that derived from other methods. However, the number of human subjects was limited (less than 30 in most of the studies). For some new sensors such as optical fibers, pyroelectric transducer, and WiFi, more validations are necessary.

The methods differ in their costs. The derivation of RR from other signals needs only the computational sources without any additional costs on hardware. The thermistor (Turnbull *et al* 2018), off-the-shelf WiFi devices (Liu *et al* 2016), paper-based humidity sensors (Güder *et al* 2016), and smartphone-based thermal imaging (Cho *et al* 2017a) are typical low-cost methods to monitor RR. The EIT, imaging and optical fiber sensors have much higher costs due to the necessity of expensive devices or components.

The methods have different applicable spatial distances. Except thermal imaging and acoustic sensors, airflow-based methods need contact with, or need to be around the mouth and nasal areas. The piezoresistive, piezoelectric and electromagnetic sensors are essentially body contact. The motion imaging and thermal imaging have the effective distance of about 3 m (Al-Naji *et al* 2017). Acoustic sensors could be body contact or non-contact. Radars and WiFi devices could detect thoracic movements at a larger distance, but under static breathing only.

There are some common limitations in the current methods. Firstly, the accurate monitoring of high and low RR values is difficult. High RR is difficult to extract from PPG signals with various algorithms (Nam *et al* 2014, Lázaro *et al* 2015). The nasal breath sound recordings by a smartphone derived the RR monitoring as high as 90 bpm (Nam *et al* 2016b). But for acoustic methods, the accuracy of low-frequency RR monitoring is influenced by environmental noise (Yabuki *et al* 2018). Considering the diagnostic significance of abnormal RR values, the accurate monitoring of high and low RR values could improve its clinical application. Secondly, the motion artifact affects the accuracy in nearly all the methods. The accurate estimation of RR during walking is difficult to derive by the FMCW radar, PPG-based method, and even the chest strap (Adib *et al* 2015). The motion artifact is also the major limitation for BCG-based (Hermann *et al* 2018), radar-based (Sun and Matsui 2015) and electromagnetic (Teichmann *et al* 2013) methods, and could decrease the accuracy of RR estimation in thermal imaging (Alkali *et al* 2017) and PPG-based (Madhav *et al* 2013) methods. Some methods have been proposed to eliminate the effects of motion artifacts, such as the model of PPG motion artefacts (Vizbara *et al* 2017), the algorithms to extract respiratory signal from PPG signals with strong motion artefacts (Madhav *et al* 2013), and the gradient in thermal imaging (Cho *et al* 2017b). Especially, the dual-accelerator could decrease the artifact by using the differential signal (Lapi *et al* 2014). Thirdly, the effect of environmental noises (or temperature) on RR results is significant in acoustic (Kim *et al* 2018, Yabuki *et al* 2018), thermal (Al-Naji *et al* 2017), and OscP-based (Chen *et al* 2016b) methods.

Clinically, the accuracy of respiration monitoring depends on the objective. The simplest devices provide estimation of respiratory rate only; more sophisticated devices will also provide quantitative information about tidal volume and gas exchange parameters. The appropriate choice of technology for respiratory monitoring will therefore take many factors into consideration: the accuracy, the cost and availability, and most importantly, the clinical condition. Towards patient-tailored treatment, the selection of appropriate devices should accord with the clinical needs.

3.2. Future directions in RR measurements

3.2.1. More accurate RR monitoring from multiple subjects

Towards the accurate RR monitoring especially for high and low RR values, besides the improvement of sensors, the data fusion could increase the estimation accuracy, as has been adopted in some studies (Yoon *et al* 2014, Shen *et al* 2017).

The simultaneous monitoring of RR on multiple human subjects could be fulfilled by using geophones (Jia *et al* 2017), WiFi devices (Wang *et al* 2016), and radar devices (Nandakumar *et al* 2015, Kocur *et al* 2017). The current methods of multiple-subject RR monitoring have some limitations. For example, the subjects must be static (Kocur *et al* 2017), or have different RR values (Wang *et al* 2016). Future research and investigation are needed towards the simultaneous real-time RR monitoring on multiple subjects based on less clinical resources, with the capability to be applied in the large-scale screening of potentially contagious patients in public places such as airports.

3.2.2. Simultaneous monitoring of physiological signals

The methods based on other signals could derive HR and RR simultaneously with the measured signals. Besides RR, the tidal volume could be derived by smartphone camera imaging (Reyes *et al* 2017) and PPG (Prinable *et al* 2017). Furthermore, the respiratory phases and time lengths could be estimated by EIT (Khodadad *et al* 2017) and FBG sensors (Massaroni *et al* 2018). The body temperature, skin humidity, and BCG could be integrated into the FBG-based or EIT-based RR monitoring straps (Fajkus *et al* 2017, Wu *et al* 2018). Minimized sensors could be fabricated in wearable T-shirts or straps to provide more comprehensive physiological information.

3.2.3. Wearable sensors

Chest straps, or belts, have become popular RR monitors as observed in piezoresistant, piezoelectric, electromagnetic, and optical sensors. The form of chest straps has extended from the traditional respiratory effort belt to those more applicable for daily use such as a short segment (Lei *et al* 2015) or safety belt (Hamdani and Fernando 2015). Besides straps, recent technical innovations have achieved RR measurement via sensors fabricated to jackets (Mahbub *et al* 2017b), T-shirts (Massaroni *et al* 2018), masks (Caccami *et al* 2017, Cao *et al* 2017), and pocket devices (Teichmann *et al* 2015). Good wearable sensors should be light, thin, and soft, with possibly less contact with skin. Some of the current wearable RR sensors are based on metallic or plastic materials, therefore inappropriate for long-term monitoring especially for infants or subjects with sensitive skin (Cao *et al* 2017). The more minimized and biocompatible wearable sensors are beneficial for long-term RR monitoring.

3.2.4. Portable sensors with wireless communication

The WiFi or radar systems are essentially appropriate for data transmission. Bluetooth (Yang *et al* 2015b, Hermann *et al* 2018), radiofrequency identification (Caccami *et al* 2017), and low power IR-UWB transmitters (Mahbub *et al* 2016, Pullano *et al* 2016) are commonly applied in wireless transmission. The smartphone could be used to perform the calculation and data transmission (Crema *et al* 2017). The portable or mobile sensors enable the RR monitoring for in-time diagnosis and first aid in acute cases. Via Bluetooth on a tablet or smartphone, the RR values can be transferred directly to available doctors who could react immediately. In the monitoring of patients at home, robust estimation of RR would assist with the management and monitoring of chronic diseases and postoperative rehabilitation.

3.3. Summary

The respiratory rate is a very important physiological parameter that is currently not well monitored in a range of healthcare settings. In the drive to attain accurate, continuous, automatic, and convenient RR monitoring, various sensor technologies have been proposed as based on various physical mechanisms.

This first review of the technologies and opportunities shows that there are many potential solutions for respiration rate measurement, based on quantifying respiratory modulation and devices measuring respiratory motions or airflow effects. However, they are mostly still at the stage of experiment or prototype. Motion artifacts and also environmental noise appear the main obstacles to clinical acceptance since they can limit the measurement accuracy. RR is worthy of the current heavy investment in resources to develop reliable sensors for long-distance measurement, remote monitoring, simultaneous measurements of multiple subjects, and capability for wearable and portable measurement, which could largely improve the reliability of the clinical daily monitoring of RR.

Acknowledgment

This work was supported by the Research Foundation of Department of Science and Technology of Guangdong Province (Grant No. 2018A050501001), and the National Natural Science Foundation of China (Grant No. 61828104).

ORCID iDs

Haipeng Liu  <https://orcid.org/0000-0002-4212-2503>

Fei Chen  <https://orcid.org/0000-0002-6988-492X>

References

- Abbasi-Kesbi R, Valipour A and Imani K 2018 Cardiorespiratory system monitoring using a developed acoustic sensor *Healthc. Technol. Lett.* **5** 7–12
- Abdelnasser H, Harras K A and Youssef M 2015 UbiBreathe: a ubiquitous non-invasive WiFi-based breathing estimator *Proc. 16th ACM Int. Symp. on Mobile Ad Hoc Networking and Computing (ACM)* pp 277–86
- Abtahi F, Snäll J, Aslamy B, Abtahi S, Seoane F and Lindecrantz K 2015 Biosignal PI, an affordable open-source ECG and respiration measurement system *Sensors* **15** 93–109
- Addison P S and Watson J N 2004 Secondary transform decoupling of shifted nonstationary signal modulation components: application to photoplethysmography *Int. J. Wavelets Multiresolut. Inf. Process.* **2** 43–57
- Addison P S, Watson J N, Mestek M L and Mecca R S 2012 Developing an algorithm for pulse oximetry derived respiratory rate (RRoxi): a healthy volunteer study *J. Clin. Monit. Comput.* **26** 45–51
- Addison P S, Watson J N, Mestek M L, Ochs J P, Uribe A A and Bergese S D 2015 Pulse oximetry-derived respiratory rate in general care floor patients *J. Clin. Monit. Comput.* **29** 113–20
- Adib F, Mao H, Kabelac Z, Katabi D and Miller R C 2015 Smart homes that monitor breathing and heart rate *Proc. 33rd Annual ACM Conf. on Human Factors in Computing Systems (ACM)* pp 837–46
- Adnane M, Jiang Z, Choi S and Jang H 2009 Detecting specific health-related events using an integrated sensor system for vital sign monitoring *Sensors* **9** 6897–912
- Alamdari N, Tavakolian K, Zakeri V, Fazel-Rezai R and Akhbardeh A 2016 A morphological approach to detect respiratory phases of seismocardiogram *Int. Conf. of the IEEE Engineering in Medicine & Biology Society* pp 4272–5
- Alkali A H, Saatchi R, Elphick H and Burke D 2017 Thermal image processing for real-time non-contact respiration rate monitoring *IET Circuits Devices Syst.* **11** 142–8
- Al-Khalidi F Q, Saatchi R, Burke D, Elphick H and Tan S 2011 Respiration rate monitoring methods: a review *Pediatr. Pulmonol.* **46** 523–9
- Al-Naji A, Gibson K, Lee S-H and Chahl J 2017 Monitoring of cardiorespiratory signal: principles of remote measurements and review of methods *IEEE Access* **5** 15776–90
- Altuve M, Carrault G, Beuchée A, Flamand C, Pladys P and Hernández A I 2012 Comparing hidden Markov model and hidden semi-Markov model based detectors of apnea-bradycardia episodes in preterm infants *Computing in Cardiology (CinC) 2012 (IEEE)* pp 389–92
- Ambekar M R and Prabhu S 2015 A novel algorithm to obtain respiratory rate from the PPG signal *Int. J. Comput. Appl.* **126** 9–12
- Atalay O, Kennon W R and Demirok E 2015 Weft-knitted strain sensor for monitoring respiratory rate and its electro-mechanical modeling *IEEE Sens. J.* **15** 110–22
- Autet L, Frasca D, Pinsard M, Cancel A, Rousseau L, Debaene B and Mimoz O 2014 Evaluation of acoustic respiration rate monitoring after extubation in intensive care unit patients *Br. J. Anaesth.* **113** 195–7
- Bahmed F, Khatoon F, Reddy B R and Bahmed F 2016 Relation between respiratory rate and heart rate—a comparative study *Indian J. Clin. Anat. Physiol.* **3** 436–9
- Bailón R, Sörnmo L and Laguna P 2006 ECG-derived respiratory frequency estimation *Advanced Methods and Tools for ECG Data Analysis* (Boston, MA: Artech House Publishers) pp 215–44
- Balasubramaniam S L, Wang Y, Ryan L, Hossain J, Rahman T and Shaffer T H 2018 Age-related ranges of respiratory inductance plethysmography (RIP) reference values for infants and children *Paediatr. Respir. Rev.* **29** 60–7
- Bao N, Wu C, Liang Q, Xu L, Li G, Qi Z, Zhang W, Ma H and Li Y 2017 The intelligent monitoring for the elderly based on WiFi signals *Pacific Rim Conf. on Multimedia (Springer)* pp 883–92
- Bates A, Ling M J, Mann J and Arvind D 2010 Respiratory rate and flow waveform estimation from tri-axial accelerometer data *2010 Int. Conf. on Body Sensor Networks (IEEE)* pp 144–50
- Bergese S D, Mestek M L, Kelley S D, McIntyre R Jr, Uribe A A, Sethi R, Watson J N and Addison P S 2017 Multicenter study validating accuracy of a continuous respiratory rate measurement derived from pulse oximetry: a comparison with capnography *Anesth. Analg.* **124** 1153–9
- Bianchi W, Dugas A F, Hsieh Y-H, Saheed M, Hill P, Lindauer C, Terzis A and Rothman R E 2013 Revitalizing a vital sign: improving detection of tachypnea at primary triage *Ann. Emerg. Med.* **61** 37–43
- Birrenkott D A, Pimentel M A, Watkinson P J and Clifton D A 2016 Robust estimation of respiratory rate via ECG- and PPG-derived respiratory quality indices *2016 IEEE 38th Annual Int. Conf. of the Engineering in Medicine and Biology Society (IEEE)* pp 676–9
- Birrenkott D A, Pimentel M A, Watkinson P J and Clifton D A 2018 A robust fusion model for estimating respiratory rate from photoplethysmography and electrocardiography *IEEE Trans. Biomed. Eng.* **65** 2033–41
- Braun F, Lemkaddem A, Moser V, Dasen S, Grossenbacher O and Bertschi M 2018 *Contactless Respiration Monitoring in Real-Time via a Video Camera* (Singapore: Springer) pp 567–70
- Bruser C, Antink C H, Wartzek T, Walter M and Leonhardt S 2015 Ambient and unobtrusive cardiorespiratory monitoring techniques *IEEE Rev. Biomed. Eng.* **8** 30–43
- Buist M, Bernard S, Nguyen T V, Moore G and Anderson J 2004 Association between clinically abnormal observations and subsequent in-hospital mortality: a prospective study *Resuscitation* **62** 137–41
- Caccami M, Mulla M, Di Natale C and Marrocco G 2017 Wireless monitoring of breath by means of a graphene oxide-based radiofrequency identification wearable sensor *2017 11th European Conf. on Antennas and Propagation (IEEE)* pp 3394–6
- Camcı B, Kahveci A Y, Arnrich B and Ersoy C 2017 Sleep apnea detection via smart phones *2017 25th Signal Processing and Communications Applications Conf. (IEEE)* pp 1–4
- Cao R, Wang J, Zhao S, Yang W, Yuan Z, Yin Y, Du X, Li N W, Zhang X and Li X 2017 Self-powered nanofiber-based screen-print triboelectric sensors for respiratory monitoring *Nano Res.* **11** 3771–9
- Cardoso F S, Karvellas C J, Kneteman N M, Meeberg G, Fidalgo P and Bagshaw S M 2014 Respiratory rate at intensive care unit discharge after liver transplant is an independent risk factor for intensive care unit readmission within the same hospital stay: a nested case-control study *J. Crit. Care* **29** 791–6

- Cernat R A, Ciorecan S I, Ungureanu C, Arends J, Strungaru R and Ungureanu G M 2015 Recording system and data fusion algorithm for enhancing the estimation of the respiratory rate from photoplethysmogram *2015 37th Annual Int. Conf. of the IEEE Engineering in Medicine and Biology Society* (IEEE) pp 5977–80
- Charlton P H, Bonnici T, Tarassenko L, Alastruey J, Clifton D A, Beale R and Watkinson P J 2017 Extraction of respiratory signals from the electrocardiogram and photoplethysmogram: technical and physiological determinants *Physiol. Meas.* **38** 669–90
- Charlton P H, Bonnici T, Tarassenko L, Clifton D A, Beale R and Watkinson P J 2016a An assessment of algorithms to estimate respiratory rate from the electrocardiogram and photoplethysmogram *Physiol. Meas.* **37** 610–26
- Charlton P H, Villarroel M and Salguiero F 2016b *Secondary Analysis of Electronic Health Records* (Berlin: Springer) pp 377–90
- Chellel A, Fraser J, Fender V, Higgs D, Buras-Rees S, Hook L, Mummery L, Cook C, Parsons S and Thomas C 2002 Nursing observations on ward patients at risk of critical illness *Nurs. Times* **98** 36–9
- Chen D, Chen F, Alan M and Zheng D 2016a Respiratory modulation of oscillometric cuff pressure pulses and Korotkoff sounds during clinical blood pressure measurement in healthy adults *Biomed. Eng. Online* **15** 53
- Chen D, Chen F, Murray A and Zheng D 2016b A method for extracting respiratory frequency during blood pressure measurement, from oscillometric cuff pressure pulses and Korotkoff sounds recorded during the measurement *Engineering in Medicine & Biology Society* p 4268
- Chen D, Chen F, Murray A and Zheng D 2016c Respiratory modulation of oscillometric cuff pressure pulses and Korotkoff sounds during clinical blood pressure measurement in healthy adults *Biomed. Eng. Online* **15** 1
- Chen D-Y and Lai J-C 2017 HHT-based remote respiratory rate estimation in thermal images *2017 18th IEEE/ACIS Int. Conf. on Software Engineering, Artificial Intelligence, Networking and Parallel/Distributed Computing* (IEEE) pp 263–8
- Chen Z, Ju T T, Ng S H and Yang X 2013 Plastic optical fiber microbend sensor used as breathing sensor *Sensors* **1**–4
- Chen Z, Lau D, Teo J T, Ng S H, Yang X and Kei P L 2014 Simultaneous measurement of breathing rate and heart rate using a microbend multimode fiber optic sensor *J. Biomed. Opt.* **19** 057001
- Cho Y, Bianchi-Berthouze N, Julier S J and Marquardt N 2017a ThermSense: Smartphone-based breathing sensing platform using noncontact low-cost thermal camera *2017 7th Int. Conf. on Affective Computing and Intelligent Interaction Workshops and Demos* (IEEE) pp 83–4
- Cho Y, Julier S J, Marquardt N and Bianchi-Berthouze N 2017b Robust tracking of respiratory rate in high-dynamic range scenes using mobile thermal imaging *Biomed. Opt. Express* **8** 4480–503
- Chung K Y, Lee B-K, Song K, Shin K, Cho S H and Chang J-H 2016 An experimental study: the sufficient respiration rate detection technique via continuous wave Doppler radar *2016 IEEE Int. Conf. on Network Infrastructure and Digital Content* (IEEE) pp 471–5
- Clifford G D, Azuaje F and McSharry P 2006 *Advanced Methods and Tools for ECG Data Analysis* (Norwood, MA: Artech House Publishers)
- Crema C, Depari A, Flammini A, Sisinni E, Vezzoli A and Bellagente P 2017 Virtual respiratory rate sensors: an example of a smartphone-based integrated and multiparametric mHealth gateway *IEEE Trans. Instrum. Meas.* **66** 2456–63
- Cretikos M A, Bellomo R, Hillman K, Chen J, Finfer S and Flabouris A 2008 Respiratory rate: the neglected vital sign *Med. J. Aust.* **188** 657–9
- Da He D, Winokur E S, Heldt T and Sodini C G 2010 The ear as a location for wearable vital signs monitoring *2010 Annual Int. Conf. of the IEEE Engineering in Medicine and Biology Society* (IEEE) pp 6389–92
- Damy T, D'ortho M P, Estrugo B, Margarit L, Mouillet G, Mahfoud M, Roudot-Thoraval F, Vermes E, Hittinger L and Roche F 2010 Heart rate increment analysis is not effective for sleep-disordered breathing screening in patients with chronic heart failure *J. Sleep Res.* **19** 131–8
- Dang V, Phan T and Kilic O 2015 Compressive sensing based approach for detection of human respiratory rate *2015 IEEE Int. Symp. on Antennas and Propagation & USNC/URSI National Radio Science Meeting* (IEEE) pp 394–5
- Das T, Guha S, Banerjee N and Basak P 2017 Development of thermistor based low cost high sensitive respiration rate measurement system using audio software with audio input *2017 3rd Int. Conf. on Biosignals, Images and Instrumentation* (IEEE) pp 1–3
- Daw W, Kingshott R, Saatchi R, Burke D, Holloway A, Travis J, Evans R, Hughes B and Elphick H 2016 Medical devices for measuring respiratory rate in children: a review *J. Adv. Biomed. Eng. Technol.* **3** 21–7
- Degner M, Jürß H and Ewald H 2018 Fast and low power optical CO₂-sensors for medical application: new sensor designs for main- and side-stream CO₂-sensors are presented in comparison with state of the art capnometers *2018 IEEE Int. Instrumentation and Measurement Technology Conf.* (IEEE) pp 1–5
- Deng F, Ye L and Song K 2014 Respiratory monitoring by a field ionization sensor based on Trichel pulses *Sensors* **14** 10381–94
- Di Marco L Y, Zheng D and Murray A 2012 Effects of deep breathing on blood pressure measurement in healthy subjects *Computing in Cardiology (CinC) 2012* (IEEE) pp 745–8
- Edmonds Z V, Mower W R, Lovato L M and Lomeli R 2002 The reliability of vital sign measurements *Ann. Emerg. Med.* **39** 233–7
- Edwards S M and Murdin L 2001 Respiratory rate—an under-documented clinical assessment *Clin. Med.* **1** 85
- Egermayer P, Town G I, Turner J G, Heaton D C, Mee A L and Beard M E 1998 Usefulness of D-dimer, blood gas, and respiratory rate measurements for excluding pulmonary embolism *Thorax* **53** 830–4
- Elstad M et al 2018 Cardiorespiratory interactions in humans and animals: rhythms for life *Am. J. Physiol.-Heart Circ. Physiol.* **315** H6–H17
- Emidio Jorge S L 2013 Respiratory rate as a predictor of weaning failure from mechanical ventilation *Braz. J. Anesthesiol.* **63** 1–12
- Erden F, Alkar A Z and Cetin A E 2015 Contact-free measurement of respiratory rate using infrared and vibration sensors *Infrared Phys. Technol.* **73** 88–94
- Ermer S, Brewer L, Kuck K and Orr J 2017 Detecting low respiratory rates using myriad, low-cost sensors *SPACEGRANT (8th May 2017)* (<https://digitalcommons.usu.edu/spacegrant/2017/Session1/3/>)
- Fajkus M, Nedoma J, Martinek R, Vasinek V, Nazeran H and Siska P 2017 A non-invasive multichannel hybrid fiber-optic sensor system for vital sign monitoring *Sensors* **17** 111
- Fajkus M, Nedoma J, Siska P and Vasinek V 2016 FBG sensor of breathing encapsulated into polydimethylsiloxane *Proc. SPIE* **9994** 99940N
- Flenady T, Dwyer T and Applegarth J 2017 Accurate respiratory rates count: So should you! *Australas. Emerg. Nurs. J.* **20** 45–7
- Frasca D, Geraud L, Charriere J M, Debaene B and Mimoz O 2015 Comparison of acoustic and impedance methods with mask capnometry to assess respiration rate in obese patients recovering from general anaesthesia *Anaesthesia* **70** 26–31
- Frerichs I, Amato M B, Van Kaam A H, Tingay D G, Zhao Z, Grychtol B, Bodenstein M, Gagnon H, Böhm S H and Teschner E 2016 Chest electrical impedance tomography examination, data analysis, terminology, clinical use and recommendations: consensus statement of the TRanslational EIT developmeNt stuDy group *Thorax* **72** 83–93
- Galle C, Papazyan J-P, Miron M-J, Slosman D, Bounameaux H and Perrier A 2001 Prediction of pulmonary embolism extent by clinical findings, D-dimer level and deep vein thrombosis shown by ultrasound *Thromb. Haemost.* **86** 1156–60
- Garde A, Karlen W, Ansermino J M and Dumont G A 2014 Estimating respiratory and heart rates from the correntropy spectral density of the photoplethysmogram *PLoS One* **9** e86427

- Gray E L and Barnes D J 2017 Beyond the thermistor: novel technology for the ambulatory diagnosis of obstructive sleep apnoea *Respirology* **22** 418–9
- Grossman P and Taylor E W 2007 Toward understanding respiratory sinus arrhythmia: relations to cardiac vagal tone, evolution and biobehavioral functions *Biol. Psychol.* **74** 263–85
- Gu C and Li C 2015 Assessment of human respiration patterns via noncontact sensing using doppler multi-radar system *Sensors* **15** 6383–98
- Güder F, Ainla A, Redston J, Mosadegh B, Glavan A, Martin T and Whitesides G M 2016 Paper-based electrical respiration sensor *Angew. Chem., Int. Ed.* **55** 5727–32
- Guechi Y, Pichot A, Frasca D, Rayeh-Pelardy F, Lardeur J-Y and Mimos O 2015 Assessment of noninvasive acoustic respiration rate monitoring in patients admitted to emergency department for drug or alcoholic poisoning *J. Clin. Monit. Comput.* **29** 721–6
- Haescher M, Matthies D J, Trimpop J and Urban B 2015 A study on measuring heart-and respiration-rate via wrist-worn accelerometer-based seismocardiography (SCG) in comparison to commonly applied technologies *Proc. 2nd Int. Workshop on Sensor-based Activity Recognition and Interaction* (ACM) p 2
- Hamdani S and Fernando A 2015 The application of a piezo-resistive cardiorespiratory sensor system in an automobile safety belt *Sensors* **15** 7742–53
- Helfenbein E, Firoozabadi R, Chien S, Carlson E and Babaeizadeh S 2014 Development of three methods for extracting respiration from the surface ECG: a review *J. Electrocardiol.* **47** 819–25
- Helliwell V, Hadfield J and Gould T 2002 Documentation of respiratory rate for acutely sick hospital in patients-An observational study *Intensive Care Medicine* (New York, NY: Springer) p S21
- Hermann S, Lombardo L, Campobello G, Burke M and Donato N 2018 A ballistocardiogram acquisition system for respiration and heart rate monitoring *2018 IEEE Int. Instrumentation and Measurement Technology Conf.* (IEEE) pp 1–5
- Hernandez J, Li Y, Reh J M and Picard R W 2014 Bioglass: Physiological parameter estimation using a head-mounted wearable device *2014 EAI 4th Int. Conf. on Wireless Mobile Communication and Healthcare (Mobihealth)* (IEEE) pp 55–8
- Hernández-Rivera D and Suaste-Gómez E 2017 Fabrication of piezoelectric PVDF/Graphene membranes by electrospinning for respiratory rate and temperature sensing *VII Latin American Congress on Biomedical Engineering CLAIB 2016 (Bucaramanga, Santander, Colombia, 26–28 October 2016)* (Springer) pp 397–400
- Hernando A, Peláez M D, Lozano M T, Aiger M, Gil E and Lázaro J 2017 Finger and forehead PPG signal comparison for respiratory rate estimation based on pulse amplitude variability *2017 25th European Signal Processing Conf. (EUSIPCO)* (IEEE) pp 2076–80
- Hochhausen N, Barbosa Pereira C, Leonhardt S, Rossaint R and Czaplik M 2018 Estimating respiratory rate in post-anesthesia care unit patients using infrared thermography: an observational study *Sensors* **18** 1618
- Hodgetts T J, Kenward G, Vlachonikolis I G, Payne S and Castle N 2002 The identification of risk factors for cardiac arrest and formulation of activation criteria to alert a medical emergency team *Resuscitation* **54** 125–31
- Hogan J 2006 Why don't nurses monitor the respiratory rates of patients? *Br. J. Nurs.* **15** 489–92
- Hu M, Zhai G, Li D, Li H, Liu M, Tang W and Chen Y 2018 Influence of image resolution on the performance of remote breathing rate measurement using thermal imaging technique *Infrared Phys. Technol.* **93** 63–9
- Huang R 2018 Contact-free breathing rate monitoring with smartphones: a sonar phase approach *PhD Thesis* Auburn University (<https://etd.auburn.edu/handle/10415/6403>)
- Hudson A 2004 Prevention of in hospital cardiac arrests—first steps in improving patient care *Resuscitation* **60** 113
- Inan O, Migeotte P F, Park K S, Etemadi M, Tavakolian K, Casanella R, Zanetti J, Tank J, Funtova I and Prisk K 2015 Ballistocardiography and seismocardiography: a review of recent advances *IEEE J. Biomed. Health Inform.* **19** 1414–27
- Jarchi D, Rodgers S J, Tarassenko L and Clifton D A 2018 Accelerometry-based estimation of respiratory rate for post-intensive care patient monitoring *IEEE Sens. J.* **18** 4981–9
- Jekova I I, Krasteva V T, Kalaydjiev A I, Mudrov T N, Ménétré S and Didon J-P 2014 Respiration detection implemented in multichannel ECG front end module: a preliminary study *Annu. J. Electron.* **8** 70–3
- Jeong J, Jang Y, Lee I, Shin S and Kim S 2009 Wearable respiratory rate monitoring using piezo-resistive fabric sensor *World Congress on Medical Physics and Biomedical Engineering (Munich, Germany, 7–12 September 2009)* (Springer) pp 282–4
- Jeyhani V, Vuorinen T, Mäntysalo M and Vehkaoja A 2017 Comparison of simple algorithms for estimating respiration rate from electrical impedance pneumography signals in wearable devices *Health Technol.* **7** 21–31
- Jia Z, Bonde A, Li S, Xu C, Wang J, Zhang Y, Howard R E and Zhang P 2017 Monitoring a person's heart rate and respiratory rate on a shared bed using geophones *Proc. 15th ACM Conf. on Embedded Network Sensor Systems* (ACM) p 6
- Jiménez D, Lobo J L, Barrios D, Prandoni P and Yusen R D 2016 Risk stratification of patients with acute symptomatic pulmonary embolism *Intern. Emerg. Med.* **29** 1–8
- Jin A, Yin B, Morren G, Duric H and Aarts R M 2009 Performance evaluation of a tri-axial accelerometry-based respiration monitoring for ambient assisted living *Annual Int. Conf. of the IEEE Engineering in Medicine and Biology Society, 2009. EMBC 2009* (IEEE) pp 5677–80
- Kano S, Dobashi Y and Fujii M 2018 Silica nanoparticle-based portable respiration sensor for analysis of respiration rate, pattern, and phase during exercise *IEEE Sens. Lett.* **2** 1–4
- Karlen W, Raman S, Ansermino J M and Dumont G A 2013 Multiparameter respiratory rate estimation from the photoplethysmogram *IEEE Trans. Biomed. Eng.* **60** 1946–53
- Kellett J, Li M, Rasool S, Green G C and Seely A 2011 Comparison of the heart and breathing rate of acutely ill medical patients recorded by nursing staff with those measured over 5 min by a piezoelectric belt and ECG monitor at the time of admission to hospital *Resuscitation* **82** 1381–6
- Khodadad D, Nordebo S, Seifnaraghi N, Waldmann A D, Müller B and Bayford R 2017 Breath detection using short-time Fourier transform analysis in electrical impedance tomography *2017 32nd General Assembly and Scientific Symp. of the Int. Union of Radio Science (URSI GASS)* (IEEE) pp 1–3
- Kim J H, Chi S I, Kim H J and Seo K-S 2018 The effect of dental scaling noise during intravenous sedation on acoustic respiration rate (RRa) *J. Dent. Anesth. Pain Med.* **18** 97–103
- Kocur D, Novák D and Demčák J 2017 A joint detection, localization and respiratory rate estimation of multiple static persons using UWB radar *2017 18th Int. Radar Symp.* (IEEE) pp 1–11
- Kogan D, Jain A, Kimbro S, Gutierrez G and Jain V 2016 Respiratory inductance plethysmography improved diagnostic sensitivity and specificity of obstructive sleep apnea *Respir. Care* **61** 1033–7
- Koyama Y, Nishiyama M and Watanabe K 2018 Smart textile using hetero-core optical fiber for heartbeat and respiration monitoring *IEEE Sens. J.* **18** 6175–80
- Lai K Y-T, Yang Y-T, Chen B-J, Shen C-J, Shiu M-F, He Z-C, Chang H-C and Lee C-Y 2014 A 3.3 V 15.6 b 6.1 pJ/0.02% RH with 10 ms response humidity sensor for respiratory monitoring *2014 IEEE Asian Solid-State Circuits Conf.* (IEEE) pp 293–6

- Lapi S, Lavorini F, Borgioli G, Calzolari M, Masotti L, Pistolesi M and Fontana G A 2014 Respiratory rate assessments using a dual-accelerometer device *Respir. Physiol. Neurobiol.* **191** 60–6
- Lázaro J, Nam Y, Gil E, Laguna P and Chon K H 2015 Respiratory rate derived from smartphone-camera-acquired pulse photoplethysmographic signals *Physiol. Meas.* **36** 2317
- Lee J and Chon K H 2010 An autoregressive model-based particle filtering algorithms for extraction of respiratory rates as high as 90 breaths per minute from pulse oximeter *IEEE Trans. Biomed. Eng.* **57** 2158–67
- Lee P J 2016 Clinical evaluation of a novel respiratory rate monitor *J. Clin. Monit. Comput.* **30** 175–83
- Lei K-F, Hsieh Y-Z, Chiu Y-Y and Wu M-H 2015 The structure design of piezoelectric poly (vinylidene fluoride)(PVDF) polymer-based sensor patch for the respiration monitoring under dynamic walking conditions *Sensors* **15** 18801–12
- Lerman J, Feldman D, Feldman R, Moser J, Feldman L, Sathyamoorthy M, Deitch K and Feldman U 2016 Linshom respiratory monitoring device: a novel temperature-based respiratory monitor *Can. J. Anesth.* **63** 1154–60
- Li B N, Dong M C and Vai M I 2010 On an automatic delineator for arterial blood pressure waveforms *Biomed. Signal Process. Control* **5** 76–81
- Li C, Peng Z, Huang T-Y, Fan T, Wang F-K, Horng T-S, Muñoz-Ferreras J-M, Gómez-García R, Ran L and Lin J 2017 A review on recent progress of portable short-range noncontact microwave radar systems *IEEE Trans. Microw. Theory Tech.* **65** 1692–706
- Lim W S, Carty S M, Macfarlane J T, Anthony R E, Christian J, Dakin K S and Dennis P M 2002 Respiratory rate measurement in adults—how reliable is it? *Respir. Med.* **96** 31–3
- Lin K-Y, Chen D-Y, Yang C, Chen K-J and Tsai W-J 2016 Automatic human target detection and remote respiratory rate monitoring 2016 *IEEE 2nd Int. Conf. on Multimedia Big Data (IEEE)* pp 354–6
- Lin Y-D, Chien Y-H and Chen Y-S 2017 Wavelet-based embedded algorithm for respiratory rate estimation from PPG signal *Biomed. Signal Process. Control* **36** 138–45
- Lindberg L-G, Ugnell H and Öberg P 1992 Monitoring of respiratory and heart rates using a fibre-optic sensor *Med. Biol. Eng. Comput.* **30** 533–7
- Liu G-z, Wu D, Mei Z-y, Zhu Q-s and Wang L 2013 Automatic detection of respiratory rate from electrocardiogram, respiration induced plethysmography and 3D acceleration signals *J. Central South Univ.* **20** 2423–31
- Liu J J, Huang M C, Xu W, Zhang X, Stevens L, Alshurafa N and Sarrafzadeh M 2015b BreathSens: a continuous on-bed respiratory monitoring system with torso localization using an unobtrusive pressure sensing array *IEEE J. Biomed. Health Inform.* **19** 1682–8
- Liu J, Wang Y, Chen Y, Yang J, Chen X and Cheng J 2015a Tracking vital signs during sleep leveraging off-the-shelf wifi *Proc. 16th ACM Int. Symp. on Mobile Ad Hoc Networking and Computing (ACM)* pp 267–76
- Liu X, Cao J, Tang S, Wen J and Guo P 2016 Contactless respiration monitoring via off-the-shelf WiFi devices *IEEE Trans. Mobile Comput.* **15** 2466–79
- Lovett P B, Buchwald J M, Stürmann K and Bijur P 2005 The vexatious vital: neither clinical measurements by nurses nor an electronic monitor provides accurate measurements of respiratory rate in triage *Ann. Emerg. Med.* **45** 68–76
- Madhav K V, Ram M R, Krishna E H, Komalla N R and Reddy K A 2013 Robust extraction of respiratory activity from PPG signals using modified MSPCA *IEEE Trans. Instrum. Meas.* **62** 1094–106
- Madsen S, Baczuk J, Thorup K, Barton R, Patwari N and Langell J T 2016 A noncontact RF-based respiratory sensor: results of a clinical trial *J. Surg. Res.* **203** 1–5
- Maharaj R, Raffaele I and Wendon J 2015 Rapid response systems: a systematic review and meta-analysis *Crit. Care* **19** 254
- Mahbub I, Hasan M S, Pullano S A, Quaiyum F, Stephens C P, Islam S K, Fiorillo A S, Gaylord M S, Lorch V and Beitel N 2015 A low power wireless apnea detection system based on pyroelectric sensor 2015 *IEEE Topical Conf. on Biomedical Wireless Technologies, Networks, and Sensing Systems (IEEE)* pp 1–3
- Mahbub I, Oh T, Shamsir S, Islam S K, Pullano S and Fiorillo A 2017a Design of a pyroelectric charge amplifier and a piezoelectric energy harvester for a novel non-invasive wearable and self-powered respiratory monitoring system 2017 *IEEE Region 10 Humanitarian Technology Conf. (R10-HTC)* (IEEE) pp 105–8
- Mahbub I, Pullano S A, Wang H, Islam S K, Fiorillo A S, To G and Mahfouz M 2017b A low-power wireless piezoelectric sensor-based respiration monitoring system realized in CMOS process *IEEE Sens. J.* **17** 1858–64
- Mahbub I, Wang H, Islam S K, Pullano S A and Fiorillo A S 2016 A low power wireless breathing monitoring system using piezoelectric transducer 2016 *IEEE Int. Symp. on Medical Measurements and Applications (IEEE)* pp 1–5
- Marques F B, Bernardino A, Jorge J and Lopes D S 2018 Estimating respiratory frequency by filtering Kinect v2 skeletal data *Annals of Medicine* (London: Taylor and Francis) pp S111–2
- Martin A and Voix J 2017 In-ear audio wearable: measurement of heart and breathing rates for health and safety monitoring *IEEE Trans. Biomed. Eng.* **6** 1256–63
- Martin-Yebra A, Landreani F, Casellato C, Pavan E, Migeotte P-F, Frigo C, Martínez J and Caiani E 2017 Evaluation of respiratory-and postural-induced changes on the ballistocardiogram signal by time warping averaging *Physiol. Meas.* **38** 1426
- Massaroni C, Venanzi C, Silvatti A P, Lo Presti D, Saccomandi P, Formica D, Giurazza F, Caponero M A and Schena E 2018 Smart textile for respiratory monitoring and thoraco-abdominal motion pattern evaluation *J. Biophotonics* **11** e201700263
- McBride J, Knight D, Piper J and Smith G B 2005 Long-term effect of introducing an early warning score on respiratory rate charting on general wards *Resuscitation* **65** 41–4
- McCutcheon E P and Rushmer R F 1967 Korotkoff sounds. An experimental critique *Circ. Res.* **20** 149–61
- McGrath S P, Pyke J and Taenzer A H 2017 Assessment of continuous acoustic respiratory rate monitoring as an addition to a pulse oximetry-based patient surveillance system *J. Clin. Monit. Comput.* **31** 561–9
- Meredith D, Clifton D, Charlton P, Brooks J, Pugh C and Tarassenko L 2012 Photoplethysmographic derivation of respiratory rate: a review of relevant physiology *J. Med. Eng. Technol.* **36** 1–7
- Miller K M, Kim A Y, Yaster M, Kudchadkar S R, White E, Fackler J and Monitto C L 2015 Long-term tolerability of capnography and respiratory inductance plethysmography for respiratory monitoring in pediatric patients treated with patient-controlled analgesia *Pediatr. Anesth.* **25** 1054–9
- Mirmohamadsadeghi L, Fallet S, Moser V, Braun F and Vesin J-M 2016 Real-time respiratory rate estimation using imaging photoplethysmography inter-beat intervals *Computing in Cardiology Conf. (CinC) 2016 (IEEE)* pp 861–4
- Mitchell G S 2004 Back to the future: carbon dioxide chemoreceptors in the mammalian brain *Nat. Neurosci.* **7** 1288–90
- Mlgaard R R, Larsen P and Håkonsen S J 2016 Effectiveness of respiratory rates in determining clinical deterioration: a systematic review protocol *JBIR Database of Syst. Rev. Implement. Rep.* **14** 19–27
- Mogera U, Sagade A A, George S J and Kulkarni G U 2014 Ultrafast response humidity sensor using supramolecular nanofibre and its application in monitoring breath humidity and flow *Sci. Rep.* **4** 4103

- Mokhlespour Esfahani M I, Narimani R and Ramezanzadehkoldeh M 2013 A wearable respiratory plethysmography using flexible sensor *Int. J. Biomed. Eng. Technol.* **11** 364–80
- Morimoto K, Tsutsui Y, Ogura S and Sunda K 2018 Are wireless electronic stethoscopes useful for respiratory rate monitoring during intravenous sedation? *J. Oral Maxillofac. Surg.* **76** 70.e1–5
- Motin M A, Karmakar C K and Palaniswami M 2017 Modified thresholding technique of MMSPCA for extracting respiratory activity from short length PPG signal 2017 39th Annual Int. Conf. of the IEEE Engineering in Medicine and Biology Society (IEEE) pp 1804–7
- Mukhopadhyay S C 2015 *Wearable Electronics Sensors: For Safe and Healthy Living*, vol 15 (Berlin: Springer)
- Nam Y, Kong Y, Reyes B, Reljin N and Chon K H 2016a Monitoring of heart and breathing rates using dual cameras on a smartphone *PLoS One* **11** e0151013
- Nam Y, Lee J and Chon K H 2014 Respiratory rate estimation from the built-in cameras of smartphones and tablets *Ann. Biomed. Eng.* **42** 885–98
- Nam Y, Reyes B A and Chon K H 2016b Estimation of respiratory rates using the built-in microphone of a smartphone or headset *IEEE J. Biomed. Health Inform.* **20** 1493–501
- Nandakumar R, Gollakota S and Watson N 2015 Contactless sleep apnea detection on smartphones *Proc. 13th Annual Int. Conf. on Mobile Systems, Applications, and Services (ACM)* pp 45–57
- Nederend I, Jongbloed M, De Geus E, Blom N and Ten Harkel A 2016 Postnatal cardiac autonomic nervous control in pediatric congenital heart disease *J. Cardiovascular Dev. Dis.* **3** 16
- Nilsson L, Goscinski T, Kalman S, Lindberg L G and Johansson A 2007 Combined photoplethysmographic monitoring of respiration rate and pulse: a comparison between different measurement sites in spontaneously breathing subjects *Acta Anaesthesiol. Scand.* **51** 1250–7
- Nurmi S, Saarensanta T, Koivisto T, Meriheinä U and Palva L 2016 Validation of an accelerometer based BCG method for sleep analysis *Technical Report Aalto University* (<https://aaltodoc.aalto.fi/handle/123456789/21176>)
- O'Brien C and Heneghan C 2007 A comparison of algorithms for estimation of a respiratory signal from the surface electrocardiogram *Comput. Biol. Med.* **37** 305–14
- Ogawa K, Koyama S, Ishizawa H, Fujiwara S and Fujimoto K 2018 Simultaneous measurement of heart sound, pulse wave and respiration with single fiber bragg grating sensor 2018 IEEE Int. Symp. on Medical Measurements and Applications (IEEE) pp 1–5
- Oh Y, Jung Y-J, Choi S and Kim D 2018 Design and evaluation of a MEMS magnetic field sensor-based respiratory monitoring and training system for radiotherapy *Sensors* **18** 2742
- Orphanidou C 2017 Derivation of respiration rate from ambulatory ECG and PPG using ensemble empirical mode decomposition: comparison and fusion *Comput. Biol. Med.* **81** 45–54
- Orphanidou C, Fleming S, Shah S A and Tarassenko L 2013 Data fusion for estimating respiratory rate from a single-lead ECG *Biomed. Signal Process. Control* **8** 98–105
- Pan J and Tompkins W J 1985 A real-time QRS detection algorithm *IEEE Trans. Biomed. Eng.* **32** 230–6
- Pandia K, Inan O T, Kovacs G T and Giovangrandi L 2012 Extracting respiratory information from seismocardiogram signals acquired on the chest using a miniature accelerometer *Physiol. Meas.* **33** 1643
- Papon M T I, Ahmad I, Saquib N and Rahman A 2015 Non-invasive heart rate measuring smartphone applications using on-board cameras: a short survey 2015 Int. Conf. on Networking Systems and Security (NSysS) (IEEE) pp 1–6
- Penzel T, McNamers J, De Chazal P, Raymond B, Murray A and Moody G 2002 Systematic comparison of different algorithms for apnoea detection based on electrocardiogram recordings *Med. Biol. Eng. Comput.* **40** 402–7
- Pimentel M A, Charlton P H and Clifton D A 2015 Probabilistic estimation of respiratory rate from wearable sensors *Wearable Electronics Sensors* (Berlin: Springer) pp 241–62
- Pimentel M A, Johnson A E, Charlton P H, Birrenkott D, Watkinson P J, Tarassenko L and Clifton D A 2017 Toward a robust estimation of respiratory rate from pulse oximeters *IEEE Trans. Biomed. Eng.* **64** 1914–23
- Ponikowski P P, Chua T P, Francis D P, Capucci A, Coats A J and Piepoli M F 2001c Muscle ergoreceptor overactivity reflects deterioration in clinical status and cardiorespiratory reflex control in chronic heart failure *Circulation* **104** 2324–30
- Ponikowski P, Chua T P, Anker S D, Francis D P, Doehner W, Banasiak W, Poole-Wilson P A, Piepoli M F and Coats A J 2001a Peripheral chemoreceptor hypersensitivity an ominous sign in patients with chronic heart failure *Circulation* **104** 544–9
- Ponikowski P, Francis D P, Piepoli M F, Davies L C, Chua T P, Davos C H, Florea V, Banasiak W, Poole-Wilson P A and Coats A J 2001b Enhanced ventilatory response to exercise in patients with chronic heart failure and preserved exercise tolerance marker of abnormal cardiorespiratory reflex control and predictor of poor prognosis *Circulation* **103** 967–72
- Presti D L, Massaroni C, Schena P S E, Formica D, Caponero M A and Di Tomaso G 2018 Smart textile based on FBG sensors for breath-by-breath respiratory monitoring: tests on women 2018 IEEE Int. Symp. on Medical Measurements and Applications (IEEE) pp 1–6
- Prinable J B, Jones P W, Thamrin C and McEwan A 2017 Using a recurrent neural network to derive tidal volume from a photoplethysmograph 2017 IEEE Life Sciences Conf. (IEEE) pp 218–21
- Prytherch D R, Smith G B, Schmidt P E and Featherstone P I 2010 VIEWS—towards a national early warning score for detecting adult inpatient deterioration *Resuscitation* **81** 932–7
- Pullano S A, Mahbub I, Bianco M G, Shamsir S, Islam S K, Gaylord M S, Lorch V and Fiorillo A S 2017 Medical devices for pediatric apnea monitoring and therapy: past and new trends *IEEE Rev. Biomed. Eng.* **10** 199–212
- Pullano S, Fiorillo A, Mahbub I, Islam S, Gaylord M and Lorch V 2016 Non-invasive integrated wireless breathing monitoring system based on a pyroelectric transducer 2016 IEEE Sensors (IEEE) pp 1–3
- Purnamaningsih R W, Widyakinanti A, Dhia A, Gumelar M R, Widiyanto A, Randy M and Soedibyo H 2018 Respiratory monitoring system based on fiber optic macro bending *AIP Conf. Proc.* **1933** 040012
- Rambaud-Althaus C, Althaus F, Genton B and D'Acremont V 2015 Clinical features for diagnosis of pneumonia in children younger than 5 years: a systematic review and meta-analysis *Lancet Infect. Dis.* **15** 439–50
- Rehouma H, Noumeir R, Jouvett P, Bouachir W and Essouri S 2017 A computer vision method for respiratory monitoring in intensive care environment using RGB-D cameras 2017 7th Int. Conf. on Image Processing Theory, Tools and Applications (IEEE) pp 1–6
- Ren L, Kong L, Foroughian F, Wang H, Theilmann P and Fathy A E 2017 Comparison study of noncontact vital signs detection using a Doppler stepped-frequency continuous-wave radar and camera-based imaging photoplethysmography *IEEE Trans. Microw. Theory Techn.* **65** 3519–29
- Reyes B A, Reljin N, Kong Y, Nam Y and Chon K H 2017 Tidal volume and instantaneous respiration rate estimation using a volumetric surrogate signal acquired via a smartphone camera *IEEE J. Biomed. Health Inform.* **21** 764–77
- Reyes B A, Reljin N, Kong Y, Nam Y, Ha S and Chon K H 2016 Towards the development of a mobile phonopneumogram: automatic breath-phase classification using smartphones *Ann. Biomed. Eng.* **44** 2746–59

- Ruangsuwana R, Velikic G and Bocko M 2010 Methods to extract respiration information from ECG signals 2010 *IEEE Int. Conf. on Acoustics Speech and Signal Processing* (IEEE) pp 570–3
- Ryan H, Cadman C and Hann L 2004 Setting standards for assessment of ward patients at risk of deterioration *Br. J. Nurs.* **13** 1186–90
- Sanyal S and Nundy K K 2018 Algorithms for monitoring heart rate and respiratory rate from the video of a user's face *IEEE J. Transl. Eng. Health Med.* **6** 1–11
- Schmidt M, Schumann A, Müller J, Bär K-J and Rose G 2017 ECG derived respiration: comparison of time-domain approaches and application to altered breathing patterns of patients with schizophrenia *Physiol. Meas.* **38** 601
- Schöbel C, Knorre S, Glos M, Garcia C, Fietze I and Penzel T 2018 Improved follow-up by peripheral arterial tonometry in CPAP-treated patients with obstructive sleep apnea and persistent excessive daytime sleepiness *Sleep Breath.* **22** 1153–60
- Selyanchyn R, Wakamatsu S, Hayashi K and Lee S-W 2015 A nano-thin film-based prototype QCM sensor array for monitoring human breath and respiratory patterns *Sensors* **15** 18834–50
- Seppä V-P, Pelkonen A S, Kotaniemi-Syrjänen A, Viik J, Mäkelä M J and Malmberg L P 2016 Tidal flow variability measured by impedance pneumography relates to childhood asthma risk *Eur. Respir. J.* **1687**–96
- Shamsir S, Hesari S H, Islam S K, Mahbub I, Pullano S and Fiorillo A 2018 Instrumentation of a pyroelectric transducer based respiration monitoring system with wireless telemetry 2018 *IEEE Int. Instrumentation and Measurement Technology Conf. (I2MTC)* (IEEE) pp 1–6
- Sharma H, Sharma K and Bhagat O L 2015 Respiratory rate extraction from single-lead ECG using homomorphic filtering *Comput. Biol. Med.* **59** 80–6
- Sharp C, Soleimani V, Hannuna S, Camplani M, Damen D, Viner J, Mirmehdi M and Dodd J W 2017 Toward respiratory assessment using depth measurements from a time-of-flight sensor *Frontiers Physiol.* **8** 65
- Shelley K H, Awad A A, Stout R G and Silverman D G 2006a The use of joint time frequency analysis to quantify the effect of ventilation on the pulse oximeter waveform *J. Clin. Monit. Comput.* **20** 81–7
- Shelley K H, Jablonka D H, Awad A A, Stout R G, Rezkanna H and Silverman D G 2006b What is the best site for measuring the effect of ventilation on the pulse oximeter waveform? *Anesth. Analg.* **103** 372–7
- Shen C-L, Huang T-H, Hsu P-C, Ko Y-C, Chen F-L, Wang W-C, Kao T and Chan C-T 2017 Respiratory rate estimation by using ECG, impedance, and motion sensing in smart clothing *J. Med. Biol. Eng.* **37** 826–42
- Shirkovskiy P, Laurin A, Chapelle D, Fink M and Ing R 2017 Contactless mapping of thoracic and abdominal motion: applications for seismocardiography 2017 *IEEE Computing in Cardiology* (IEEE) pp 1–4
- Sifuentes E, Cota-Ruiz J and González-Landaeta R 2016 Respiratory rate detection by a time-based measurement system *Rev. Mex. Ing. Bioméd.* **37** 91–9
- Smith A F and Wood J 1998 Can some in-hospital cardio-respiratory arrests be prevented? A prospective survey *Resuscitation* **37** 133–7
- Sowho M, Amatoury J, Kirkness J P and Patil S P 2014 Sleep and respiratory physiology in adults *Clin. Chest Med.* **35** 469–81
- Subbe C P, Kruger M, Rutherford P and Gemmel L 2001 Validation of a modified Early Warning Score in medical admissions *QJM* **94** 521–6
- Subbe C, Davies R, Williams E, Rutherford P and Gemmell L 2003 Effect of introducing the modified early warning score on clinical outcomes, cardio-pulmonary arrests and intensive care utilisation in acute medical admissions *Anaesthesia* **58** 797–802
- Sun G and Matsui T 2015 Rapid and stable measurement of respiratory rate from Doppler radar signals using time domain autocorrelation model 2015 *37th Annual Int. Conf. of the IEEE Engineering in Medicine and Biology Society* (IEEE) pp 5985–8
- Sun G, Matsui T, Watai Y, Kim S, Kirimoto T, Suzuki S and Hakozaaki Y 2018 Vital-SCOPE: design and evaluation of a smart vital sign monitor for simultaneous measurement of pulse rate, respiratory rate, and body temperature for patient monitoring *J. Sens.* **2018** 4371872
- Sun Y and Thakor N 2016 Photoplethysmography revisited: from contact to noncontact, from point to imaging *IEEE Trans. Biomed. Eng.* **63** 463–77
- Tanaka P P, Tanaka M and Drover D R 2014 Detection of respiratory compromise by acoustic monitoring, capnography, and brain function monitoring during monitored anesthesia care *J. Clin. Monit. Comput.* **28** 561–6
- Tavel M E, Faris J, Nasser W K, Feigebaum H and Fisch C 1969 Korotkoff sounds. Observations on pressure-pulse changes underlying their formation *Circulation* **39** 465–74
- Teichmann D, De Matteis D, Bartelt T, Walter M and Leonhardt S 2015 A bendable and wearable cardiorespiratory monitoring device fusing two noncontact sensor principles *IEEE J. Biomed. Health Inform.* **19** 784–93
- Teichmann D, Foussier J, Jia J, Leonhardt S and Walter M 2013 Noncontact monitoring of cardiorespiratory activity by electromagnetic coupling *IEEE Trans. Biomed. Eng.* **60** 2142–52
- Touw H R, Verheul M H, Tuinman P R, Smit J, Thöne D, Schober P and Boer C 2017 Photoplethysmography respiratory rate monitoring in patients receiving procedural sedation and analgesia for upper gastrointestinal endoscopy *J. Clin. Monit. Comput.* **31** 747–54
- Trimpop J, Schenk H, Bieber G, Lämmel F and Burggraf P 2017 Smartwatch based respiratory rate and breathing pattern recognition in an end-consumer environment *Proc. 4th Int. Workshop on Sensor-based Activity Recognition and Interaction* (ACM) p 4
- Trobec R, Rashkovska A and Avbelj V 2012 Two proximal skin electrodes—a respiration rate body sensor *Sensors* **12** 13813–28
- Turnbull H, Kasereka M C, Amirav I, Sahika S E, Solomon I, Aldar Y and Hawkes M T 2018 Development of a novel device for objective respiratory rate measurement in low-resource settings *BMJ Innov.* **4** 185–91
- Ur A and Gordon M 1970 Origin of Korotkoff sounds *Am. J. Physiol.* **218** 524–9
- Vainer B G 2018 A novel high-resolution method for the respiration rate and breathing waveforms remote monitoring *Ann. Biomed. Eng.* **46** 960–71
- Van Loon K, Breteler M, Van Wolfwinkel L, Leyssius A R, Kossen S, Kalkman C, van Zaane B and Peelen L 2016 Wireless non-invasive continuous respiratory monitoring with FMCW radar: a clinical validation study *J. Clin. Monit. Comput.* **30** 797–805
- Vehkaoja A, Kontunen A and Lekkala J 2015 Effects of sensor type and sensor location on signal quality in bed mounted ballistocardiographic heart rate and respiration monitoring 2015 *37th Annual Int. Conf. of the IEEE Engineering in Medicine and Biology Society* (IEEE) pp 4383–6
- Venet R, Miric D, Pavie A and Lacheheb D 2000 Korotkoff sound: the cavitation hypothesis *Med. Hypotheses* **55** 141–6
- Vizbara V, Sokas D and Marozas V 2017 Motion artifacts in photoplethysmographic signals modeling based on optical and topological properties of skin *Biomed. Eng.* **20** 171–4
- Wang H, Zhang D, Ma J, Wang Y, Wang Y, Wu D, Gu T and Xie B 2016 Human respiration detection with commodity wifi devices: do user location and body orientation matter? *Proc. 2016 ACM Int. Joint Conf. on Pervasive and Ubiquitous Computing* (ACM) pp 25–36
- Wang S, Liu M, Pang B, Li P, Yao Z, Zhang X and Chen H 2018 A new physiological signal acquisition patch designed with advanced respiration monitoring algorithm based on 3-axis accelerator and gyroscope 2018 *40th Annual Int. Conf. of the IEEE Engineering in Medicine and Biology Society* (IEEE) pp 441–4

- Wartzek T, Weyer S and Leonhardt S 2011 A differential capacitive electrical field sensor array for contactless measurement of respiratory rate *Physiol. Meas.* **32** 1575
- Williams B, Alberti G, Ball C, Bell D, Binks R and Durham L 2012 *National Early Warning Score (NEWS): Standardising the Assessment of Acute-Illness Severity in the NHS* (London: The Royal College of Physicians)
- Witt J, Narbonneau F, Schukar M, Krebber K, De Jonckheere J, Jeanne M, Kinet D, Paquet B, Depre A and Dangelo L T 2012 Medical textiles with embedded fiber optic sensors for monitoring of respiratory movement *IEEE Sens. J.* **12** 246–54
- Wolf G K and Arnold J H 2005 Noninvasive assessment of lung volume: respiratory inductance plethysmography and electrical impedance tomography *Crit. Care Med.* **33** S163–9
- Wu Y, Jiang D, Bardill A, de Gelidi S, Bayford R and Demosthenous A 2018 A high frame rate wearable EIT system using active electrode ASICs for lung respiration and heart rate monitoring *IEEE Trans. Circuits Syst.* **65** 1–11
- Xue H, Yang Q, Wang D, Luo W, Wang W, Lin M, Liang D and Luo Q 2017 A wearable pyroelectric nanogenerator and self-powered breathing sensor *Nano Energy* **38** 147–54
- Yabuki S, Toyama H, Takei Y, Wagatsuma T, Yabuki H and Yamauchi M 2018 Influences of environmental noise level and respiration rate on the accuracy of acoustic respiration rate monitoring *J. Clin. Monit. Comput.* **32** 127–32
- Yan H, Zhang L, Yu P and Mao L 2016 Sensitive and fast humidity sensor based on a redox conducting supramolecular ionic material for respiration monitoring *Anal. Chem.* **89** 996–1001
- Yang J, Chen B, Zhou J and Lv Z 2015a A low-power and portable biomedical device for respiratory monitoring with a stable power source *Sensors* **15** 19618–32
- Yang X, Chen Z, Elvin C S M and Lam H Y J 2015b Textile fiber optic microbend sensor used for heartbeat and respiration monitoring *IEEE Sens. J.* **15** 757–61
- Yasuma F and Hayano J 2004 Respiratory sinus arrhythmia: why does the heartbeat synchronize with respiratory rhythm? *Chest* **125** 683–90
- Yoon J-W, Noh Y-S, Kwon Y-S, Kim W-K and Yoon H-R 2014 Improvement of dynamic respiration monitoring through sensor fusion of accelerometer and gyro-sensor *J. Electr. Eng. Technol.* **9** 334–43
- Zakeri V, Akhbardeh A, Alamdari N, Fazel-Rezai R, Paukkunen M and Tavakolian K 2016 Analyzing seismocardiogram cycles to identify the respiratory phases *IEEE Trans. Biomed. Eng.* **64** 1786–92
- Zhang X and Ding Q 2016 Respiratory rate monitoring from the photoplethysmogram via sparse signal reconstruction *Physiol. Meas.* **37** 1105
- Zhang X, Kassem M A M, Zhou Y, Shabsigh M, Wang Q and Xu X 2017 A brief review of non-invasive monitoring of respiratory condition for extubated patients with or at risk for obstructive sleep apnea after surgery *Frontiers Med.* **4** 26
- Zhang Z, Zheng J, Wu H, Wang W, Wang B and Liu H 2012 Development of a respiratory inductive plethysmography module supporting multiple sensors for wearable systems *Sensors* **12** 13167–84
- Zheng D, Di Marco L Y and Murray A 2014 Effect of respiration on Korotkoff sounds and oscillometric cuff pressure pulses during blood pressure measurement *Med. Biol. Eng. Comput.* **52** 467–73